Bioorganic Chemistry xxx (xxxx) 105380

Contents lists available at ScienceDirect

Bioorganic Chemistry

journal homepage: www.elsevier.com/locate/bioorg

Amberlyst-15 catalysed synthesis of novel indole derivatives under ultrasound irradiation: Their evaluation as serotonin 5-HT_{2C} receptor agonists

Gangireddy Sujeevan Reddy [a, b], Rajamanikkam Kamaraj [a], Kazi Amirul Hossain [c], Jetta Sandeep Kumar [a, b], Raghavender Medishetti [a, b], N. Sushma Sri [a], Parimal Misra [a], Manojit Pal [a, *]

[a] Dr Reddy's Institute of Life Sciences, University of Hyderabad Campus, Gachibowli, Hyderabad 500 046, India
[b] Manipal College of Pharmaceutical Sciences, Manipal Academy of Higher Education, Madhav Nagar, Manipal 576 104, Karnataka, India
[c] Department of Physical Chemistry, Gdansk University of Technology, ul. Narutowicza 11/12, 80-233 Gdansk, Poland

ARTICLE INFO

Keywords:
Indole
Schiff base
Ultrasound
Agonist
5-HT2C receptor

ABSTRACT

A series of indole based novel Schiff bases was designed as potential agonists of 5-HT_{2C} receptor that was supported by docking studies *in silico*. These compounds were synthesized via Amberlyst-15 catalysed condensation of an appropriate pyrazole based primary amine with the corresponding indole-3-aldehyde under ultrasound irradiation at ambient temperature. A number of target Schiff bases were obtained in good yields (77–87%) under mild conditions within 1 h. Notably, the methodology afforded the corresponding pyrazolo[4,3-*d*]pyrimidin-7(4H)-one derivatives when the primary amine was replaced by a secondary amine. Several Schiff bases showed agonist activity when tested against human 5-HT_{2C} using luciferase assay in HEK293T cells *in vitro*. The SAR (Structure-Activity-Relationship) studies suggested that the imine moiety was more favorable over its cyclic form i.e. the corresponding pyrazolopyrimidinone ring. The Schiff bases **3b** (EC_{50} 1.8 nM) and **3i** (EC_{50} 5.7 nM) were identified as the most active compounds and were comparable with Lorcaserin (EC_{50} 8.5 nM). Also like Lorcaserin, none of these compounds were found to be PAM of 5-HT_{2C}. With ~24 and ~150 fold selectivity towards 5-HT_{2C} over 5-HT_{2A} and 5-HT_{2B} respectively the compound **3i** that reduced locomotor activity in zebrafish (Danio rerio) larvae model emerged as a promising hit molecule for further study.

1. Introduction

The serotonin (5-hydroxytryptamine, 5-HT) receptor family has long been known to play an important role in modulating the food intake [1–3] in addition to several other physiological functions. Indeed, raising the level of serotonin is known to be the mechanism of action of the classical anti-obesity drugs such as dexfenfluramine and sibutramine [2,3]. There are several subtypes known for this GPCR (G protein-coupled receptor) family that are classified into seven main classes e.g. 5-$HT_{1\text{-}7}$. Notably, the 5-HT_3 belongs to ion-channel coupled receptor class. The 5-HT_2 class on the other hand has three members called 5-HT_{2A}, 5-HT_{2B} and 5-HT_{2C} possessing a close sequence of homology. The GPCR 5-HT_{2C} being broadly distributed in various regions of brain is largely expressed in the central nervous system (CNS) and involved in numerous physiological functions. Indeed, the modulation of this GPCR has been thought to have beneficial effects in a number of pathological conditions in addition to obesity [4–6]. While agonists and antagonists of 5HT_{2C} have been studied and reported in the literature the former class of ligands were considered as the most promising agents for the control of food intake thereby body weight reduction mediated by serotonin [7–9]. The success of 5HT_{2C}R agonist was culminated by the launching of anti-obesity drug Lorcaserin ([1R]-8-chloro-2,3,4,5-tetrahydro-1-methyl-1*H*-3-benzazepine or Belviq) [10,11]. Indeed, Lorcaserin was reported to reduce body weight by decreasing energy intake without influencing energy expenditure. However, a weight loss of only 3.0–3.6% per year compared to placebo was observed with the use of Lorcaserin [12]. Additionally, this drug was known to cause cardiovascular side effects in addition to several other problems [13]. Moreover, due to an increased risk of cancer (emerged from a safety clinical trial) the FDA in February 2020 requested the manufacturer of Lor-

* Corresponding author.
E-mail address: manojitpal@rediffmail.com (M. Pal).

https://doi.org/10.1016/j.bioorg.2021.105380
Received 23 May 2021; Received in revised form 7 July 2021; Accepted 19 September 2021
0045-2068/

caserin to voluntarily withdraw the drug from the US market [14]. While the reason for its cancer risk is not clear the study suggested that the other main side effects of Lorcaserin are related to its subtype selectivity because activation of 5-HT_{2A} and 5-HT_{2B} are known to be associated with potential hallucinogenic effects [15] and cardiac valvulopathy [16,17], respectively. Additionally, the common adverse effects such as headache, flushing, nausea, hypotension etc are known to be associated with the benzazepine class of drugs such as Fenoldopam. However, the modest effectiveness of Lorcaserin in addition to its side effects rather than the possibility of increased cancer risk might be the main reason for its withdrawal. Thus, it is desirable to devote efforts in the discovery and development of alternative class of anti-obesity agents based on a new chemotype that may show better effects on body weight with lower side effects.

Recently, an indole derivative **A** (Fig. 1) has been identified as a Positive Allosteric Modulator (PAM) of 5-HT_{2C}R for the potential treatment of obesity [18a]. The compound **A** showed dose-dependent increase of serotonin efficacy, no serious off-target effects, and low binding competition with serotonin or other orthosteric ligands. Moreover, according to another recent report several indole derivatives have shown moderate-to-strong preferences for activation of the 5-HT_{2C} subtype at nanomolar concentrations [18b]. These reports and the impressive and favorable pharmacological properties of **A** prompted us to design, synthesize and assess 5-HT_{2C}R agonism of a new series of indole derivatives based on the framework **C** (Fig. 1). Our design initially involved replacing the C—N bond and the pyridine ring of **A** by the C═N moiety [18c] and a heteroaryl group respectively to afford the framework **B** (Fig. 1). Since a number of compounds could be derived from **B** by varying the heteroaryl group hence we focused on substituted pyrazole ring possessing an amide and alkyl group at this stage. Our strategy was backed by the fact that amide class of compounds were already explored as orally active and brain permeable selective $5HT_{2C}$ agonists for the treatment of obesity [19a] whereas $5HT_{2C}$ agonistic properties of pyrazole class of molecules are known in the literature [19b]b]. Additionally, the 5-HT_{2A} agonism [18c] and anti-obesity potential [20] of Schiff bases has also been explored earlier. Thus, the framework **C** (Fig. 1) after introducing the substituents R^1 and R^2 (to induce further diversity) was chosen to build a library of molecules for pharmacological evaluation.

To verify the merit and potential of our current designing approach, the docking study of two representative molecules e.g. **C-1** and **C-2** along with Lorcaserin and serotonin was performed against the $5HT_{2C}$R (PDB ID: 6BQG) using AutoDock Vina [21]. The interaction diagrams are presented in Figs. 2-4 (see also Fig S-1, S-2 and S-3 for enlarged figure in Suppl data) in and the docking scores are summarized in Chart 1. It is worthy to mention that due to the random sampling process (e.g. Lamarckian Genetic Algorithm (LGA) and rough estimation of docking score, the obtained scores were mostly used for the comparative analysis purpose (as the absolute value may reflects the over stabilized binding). Recently, Roth, Stevens, Liu and co-workers [22a] solved the crystal structure of $5HT_{2C}$R in the presence of non-selective agonist Ergotamine as well as selective inverse agonist Ritanserin. Their studies allowed identification as well as differentiation of binding site residues

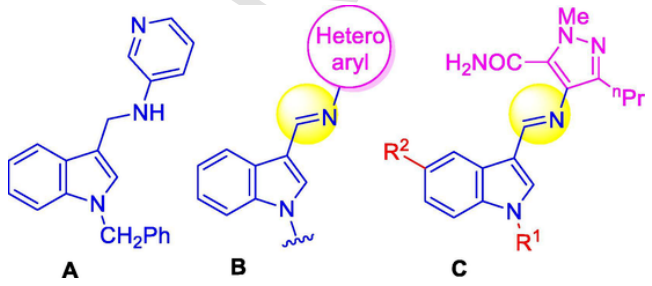

Fig. 1. Reported indole derivative **A** and the new template **B** and **C**.

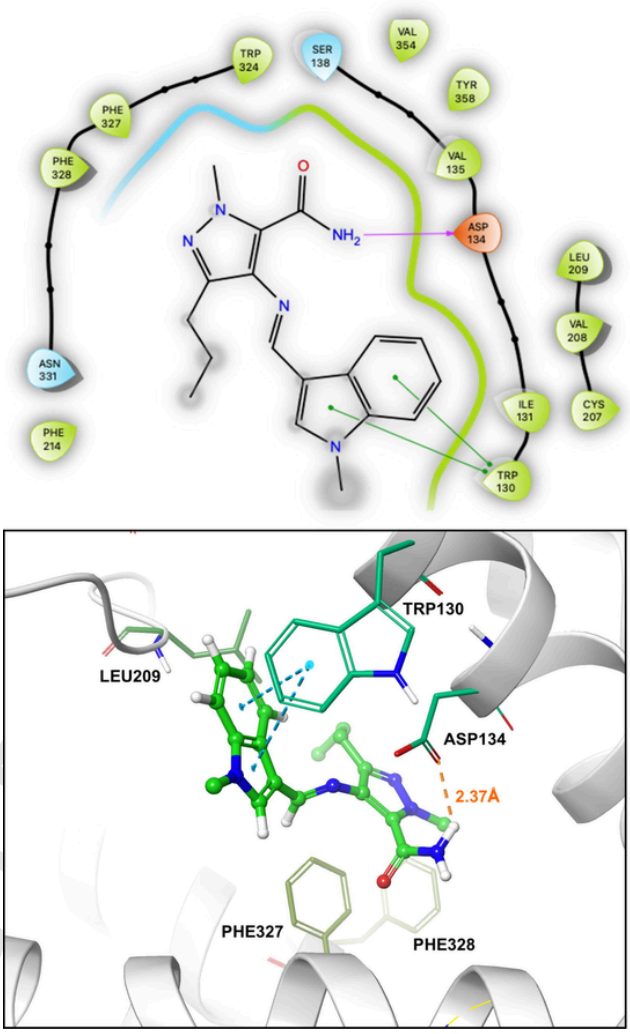

Fig. 2. The 2D and 3D interaction diagram between orthosteric binding site residues of $5HT_{2C}$R and **C-1**, which are prepared in Maestro visualizer (Schrödinger, LLC), (the H-bond and pi-pi interaction is shown as magenta and green line, respectively in 2D diagram and orange as well as dotted cyan in 3D diagram). (For interpretation of the references to color in this figure legend, the reader is referred to the web version of this article.)

crucial for agonism and inverse-agonism. In case of current study, the interaction diagram (Fig. 2) indicated agonistic activity of the molecule **C-1** because like Ergotamine it showed the similar H-bond interaction with the conserved Asp134$^{3.32}$ at a distance of 2.37 Å (the figure presented in superscript font indicate Ballesteros–Weinstein numbering [22b-e]), and hydrophobic/van der Waals contact with other important residues such as Phe327$^{6.51}$&328$^{6.52}$, and Trp324$^{6.48}$. Moreover, the indole ring of **C-1** was involved in pi-pi interaction with Trp130$^{3.28}$ and several other non-bonded contacts (like hydrophobic or van der Waals interactions) with hydrophobic residues Ile131, Leu209, Val208, Cys207, etc. Notably, **C-1** avoided the interactions with Phe223 and Phe320 that were observed in case of inverse-agonist like Ritanserin. Like **C-1** the molecule **C-2** also interacted with $5HT_{2C}$R *via* hydrophobic and van der Waals contacts (Fig. 3). Indeed, additional hydrophobic contacts with residues Phe214$^{5.38}$, Leu350$^{7.35}$, Leu209^{EL2}, Val354$^{7.39}$ etc were observed in case of **C-2** involving its benzyl moiety. However, it formed the H-bond with Asp134 within a shorter distance (i.e. 1.9 Å) compared to that of **C-1**, and pi-pi interaction with another important conserved residue Phe328. Moreover, it showed contacts with residues Trp130, Phe327, Trp324, Val135$^{3.33}$ etc. It is evident from Chart 1 that both the molecules showed docking scores comparable to the reference

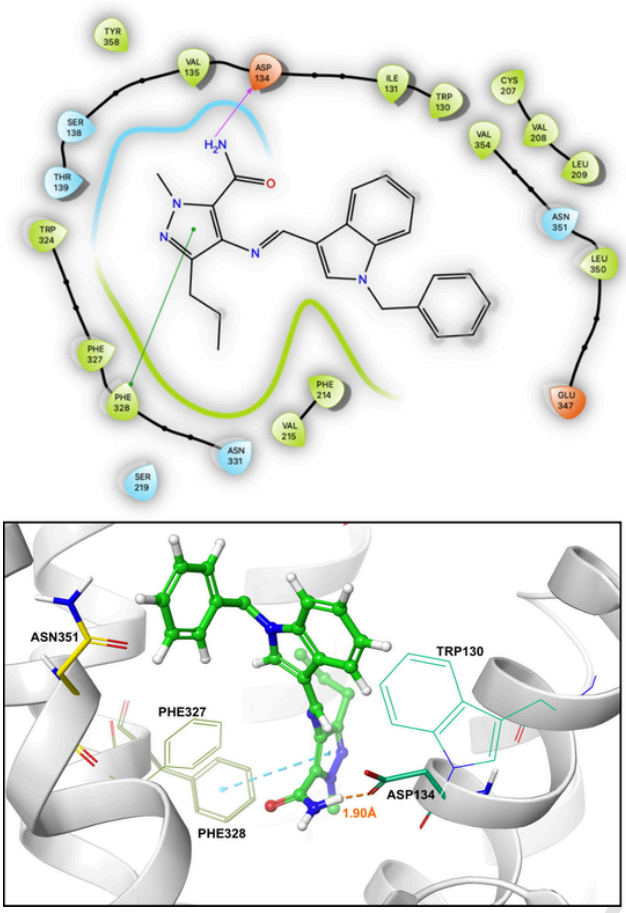

Fig. 3. 2D followed by 3D interaction diagram between orthosteric binding site residues of $5HT_{2C}R$ and **C-2**.

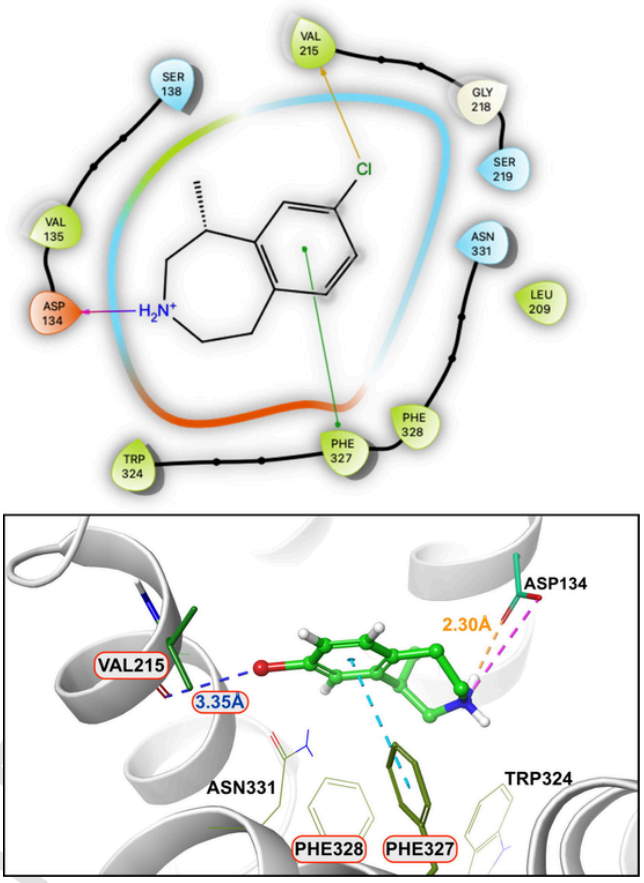

Fig. 4. 2D followed by 3D interaction diagram between orthosteric binding site residues of $5HT_{2C}R$ and Lorcaserin [the halogen bond between the Cl group of Lorcaserin and Val215 is shown in yellow and blue color in 2D and 3D diagram, respectively. The pi-pi stacking in green and cyan (for 2D and 3D respectively), the H-bond (of salt-bridge) in purple and orange (for 2D & 3D), the electrostatic interaction of salt-bridge shown in pink dotted line in the 3D interaction diagram]. (For interpretation of the references to color in this figure legend, the reader is referred to the web version of this article.)

compound Lorcaserin **L** and serotonin **S** suggesting their possible encouraging interactions with the $5HT_{2C}R$. Indeed, with the docking score of −10.7 kcal/mol the compound **C-2** emerged as a promising and potential agent from this *in silico* study. The possible reasons for higher score of **C-2** over **C-1** were due to its participation in the additional hydrophobic contacts and more importantly in the H-bond formation at a shorter distance. Similarly, Lorcaserin though showed the conserved salt-bridge with Asp134 (at a distance 2.3 Å) and the agonistic aromatic pi interaction with the residue Phe327 (Fig. 4) but unlike **C-1** and **C-2** it showed a fewer number of hydrophobic contacts with residues Trp324, Phe328, Leu209 etc. Additionally, it formed a halogen-bond involving its Cl group and the backbone of Val215. While serotonin (the endogenous ligand of the receptor) formed a salt-bridge and H-bond with Asp134 and Ser219, respectively however like Lorcaserin it also lacked several non-bonded contacts and participated in a less number of hydrophobic contacts with residues Phe328, Phe327, Tyr358$^{7.43}$, Phe214 etc (see Fig S-4 in suppl data). Overall, all these observations encouraged us to synthesize and evaluate a series of novel Schiff bases based on **C** as potential agonists of 5-HT_{2C} receptor.

2. Results and discussion

2.1. Chemistry

The designed indole based Schiff bases were conveniently prepared by condensation of one mole of appropriate pyrazole amine (**1a**) with 1.1 mol of the corresponding indole-3-aldehyde (**2**) (Scheme 1). Traditionally, Schiff bases are often prepared *via* acid-catalysed condensation of amines with an aldehyde (or ketone) in a suitable organic media under refluxing conditions [23]. For example, synthesis of indole-pyrazole Schiff bases required refluxing (at 80 °C) in EtOH for 15–18 h in the presence of HCl [23b]. Nevertheless, *p*-toluene sulfonic acid (PTSA) is commonly used for the preparation of Schiff bases [23c] and being a homogenous catalyst PTSA is not recoverable. The heterogeneous catalysts on the other hand being recoverable and recyclable agents have certain advantages over the homogenous catalysts and played a central role in various organic transformations [24]. As an inexpensive and commercially available heterogeneous catalyst Amberlyst-15 attracted our interest [25–29] due to its non-hazardous nature and easy removal from the reaction mixture, for example, *via* simple filtration [30]. Over the years the ultrasound-mediated methods have emerged as one of the common approaches in organic synthesis which is apparent from a range of applications of these methodologies in the preparation of various compounds and agents [31]. The features and benefits of these reactions include their (i) involvement as green approaches in organic

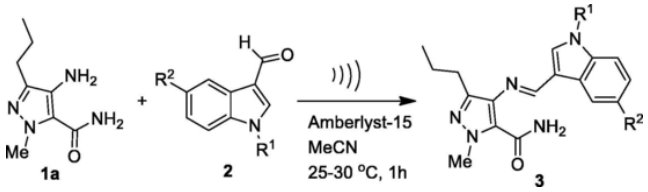

Scheme 1. Synthesis of indole derivatives **3**.

synthesis [32], (ii) reduction of waste generation as well as energy requirements [33] and (iii) efficiency and effectiveness for the synthesis of desired products *via* employing shorter reaction time and milder conditions at the same time increasing the product yields [34,35]. As part of our ongoing effort in the use of ultrasound as an alternative source of energy and Amberlyst-15 as a user-friendly heterogeneous catalyst in various organic reactions we became interested in exploring these reaction conditions in our current endeavor. Thus the ultrasound assisted condensation of primary amine **1a** with the aldehyde **2** was carried out in the presence of Amberlyst-15 under mild conditions to give the desired product **3** in good yields (Scheme 1). Notably, to the best of our knowledge the use of combination of Amberlyst-15 and ultrasound for the synthesis of Schiff bases is not common in the literature.

Table 1
Effect of reaction conditions on condensation of amine (**1**) with aldehyde (**2a**).[a]

Entry	Catalyst	Solvent	T (°C)	Yield[b]
	PTSA	Toluene	110–115	67[c]
	Amberlyst-15	Toluene	110–115	62[c]
	Amberlyst-15	MeCN	25–30	77
	Amberlyst-15	MeCN	25–30	79[d]
	Amberlyst-15	MeOH	25–30	71
	Amberlyst-15	DCM	25–30	70
	Amberlyst-15	THF	25–30	65
	Amberlyst-15	H_2O	25–30	34
	No catalyst	MeCN	25–30	11

[a] All reactions were carried out using the amine **1a** (1 mmol.), aldehyde **2a** (1.1 mmol), and a catalyst in a solvent (5.0 mL) under ultrasound irradiation for 1 h.
[b] Isolated yields.
[c] The reaction was performed in the absence of ultrasound for 12 h.
[d] The reaction was performed for 6 h.

Initially, the pyrazole amine **1a** was reacted with the indole-3-aldehyde (**2a**) in the presence of PTSA (catalytic amount) in toluene at refluxing temperature (110–115 °C) for 12 h when the desired product **3a** was obtained in 67% yield (entry 1, Table 1). The product yield was not improved when PTSA was replaced by the heterogeneous catalyst Amberlyst-15 (entry 2, Table 1). However, an increase in yield of **3a** was observed when the reaction was performed under ultrasound irradiation using a laboratory ultrasonic bath SONOREX SUPER RK 510H model producing irradiation of 35 kHz (entry 3, Table 1). Indeed, the reaction proceeded at 25–30 °C and afforded the desired product **3a** within 1 h. Encouraged by this observation we carried out the reaction for a longer duration i.e. 6 h however no significant improvement in product yield was observed (entry 4, Table 1). The use of other solvents such as MeOH, DCM (dichloromethane), THF and pure water was examined and found to be less effective under the conditions employed (entries 5–8, Table 1). Notably the reaction did not proceed well in the absence of Amberlyst-15 indicating the key role played by the catalyst in the current Schiff base formation reaction (entry 9, Table 1). Overall, the combination of Amberlyst-15, ultrasound and MeCN was found to be most effective for the preparation of **3a** and therefore used for the preparation of its other related analogues (Scheme 1, Table 2, see also Table S-1, suppl data). A number of indole-3-aldehydes (**2**) were reacted with the primary amine **1a** under the optimized conditions. The reaction proceeded well irrespective of the presence of various substituents on the indole nitrogen affording the desired indole based Schiff bases (**3b-i**, **3k** and **3l**) in good yields. The product **3j** having no substituent on indole nitrogen was also obtained in good yield in addi-

Table 2
Amberlyst-15 catalyzed synthesis of indole based Schiff bases (**3**) under ultrasound irradiation[a,b] (Scheme 1).

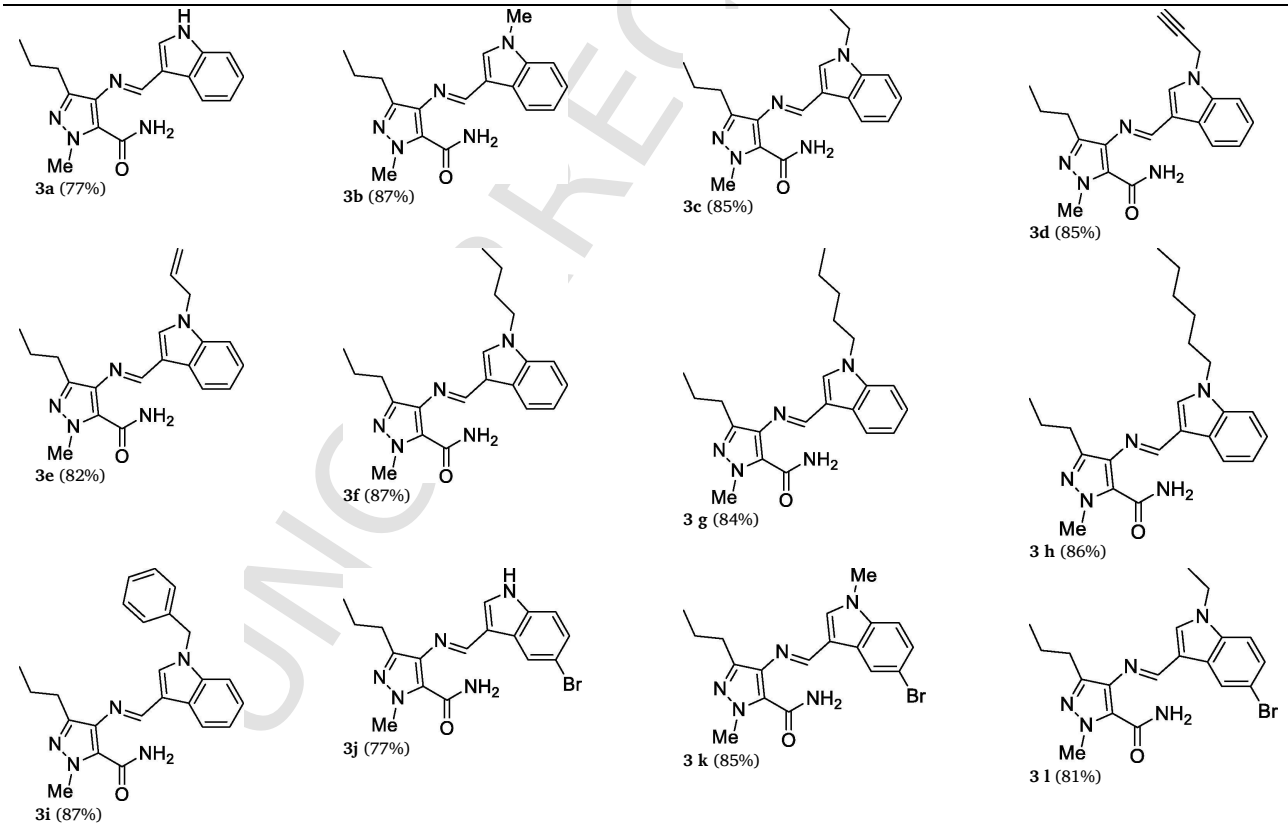

[a] All reactions were carried out using the amine **1a** (1 mmol.), aldehyde **2** (1.1 mmol), and Amberlyst-15 (10% w/w) in MeCN (5.0 mL) under ultrasound irradiation for 1 h.
[b] Figure in the bracket represents isolated yield.

tion to **3a**. Notably, the use of a secondary amine (**1b**) in the current Amberlyst-15 catalyzed condensation reaction under ultrasound afforded the corresponding 5,6-dihydro-1*H*-pyrazolo[4,3-*d*]pyrimidin-7(4*H*)-one derivatives (**4**) in high yield (Scheme 2). This was not surprising because the corresponding Schiff bases if formed were not expected to be stable in these cases and therefore favored the intramolecular cyclization involving the proximate amide moiety (see the mechanistic discussion).

All the synthesized Schiff bases and pyrazolo[4,3-*d*]pyrimidin-7(4*H*)-one derivatives (**3** and **4**) were characterized by (^{1}H and ^{13}C NMR, and MS) spectral data. Briefly (see Table S-2A in the suppl data), a singlet near δ8.7 and 8.1 in the ^{1}H NMR spectra accounted for the linker imine proton [23b] and C-2 hydrogen of the indole ring, respectively. The compound **3** was further characterized by the presence of NCH_3 protons near δ 4.0 and the *n*-propyl chain near δ 2.7 (t, CH_2), 1.7–1.6 (m, CH_2) and 0.9 (t, CH_3). The "C═O" group of the amide moiety appeared near 161 ppm in ^{13}C NMR spectra of compound **3**. In case of compound **4** the presence of 5,6-dihydro-1*H*-pyrazolo[4,3-*d*]pyrimidin-7(4*H*)-one ring was indicated by the appearance of a doublet near δ 5.9 due to the C-5 proton in their ^{1}HNMR spectra. This was further supported by the ^{13}C signal observed at 158 and 68 ppm due to the amide carbonyl and C-5 carbon of the same ring, respectively. Finally, the *E*-geometry of –N═C- of **3** was supported by (i) HPLC data (single isomer, purity ≥ 95%) and (ii) correlation of ^{1}HNMR data of **3** with the reported indole-pyrazole Schiff bases for which the *E*-geometry was confirmed by single crystal X-ray analysis [23b] (see Table S-2B in the suppl data).

Based on the fact that the reaction of a carbonyl compound with an amine is greatly facilitated by Amberlyst-15 [36], a plausible mechanism [36–38] for the current ultrasound assisted reaction [39] may be outlined as follows: (i) activation of aldehyde **2** followed by (ii) condensation with the amine **1** to generate an iminium intermediate *in situ*

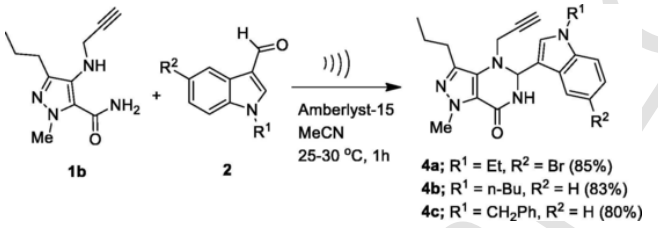

Scheme 2. The Amberlyst-15 catalyzed condensation of secondary amine (**1b**) with indole-3-aldehydes (**2**) under ultrasound.

which either afford (iii) the Schiff base **3** or the product **4** with the regeneration of the catalyst to complete the catalytic cycle (for further details see suppl data, Scheme S-1).

2.2. Biology

Having synthesized a number of Schiff bases (**3a-l**) and then three pyrazolo[4,3-*d*]pyrimidin-7(4*H*)-one derivatives (**4a-c**) all these indole based compounds were screened against human 5-HT_{2C} for agonist activity using luciferase assay in HEK293T cells *in vitro* [40,41]. Initially, the fold stimulation was measured for all the compounds at a concentration of 10 μM using Lorcaserin as a reference compound and results are presented in Fig. 5. It is evident from Fig. 5 that several Schiff bases e.g. **3d**, **3e**, **3j, 3k, 3l** etc showed moderate to reasonable activities (≤2 fold stimulation) compared to Lorcaserin (≥2 fold stimulation) whereas **3b** and **3i** were found to be promising (>2 and 3 fold response, respectively) based on multiple comparison result. Notably, all the pyrazolo[4,3-*d*]pyrimidin-7(4*H*)-one derivatives (**4a-c**) showed low activity indicating that the omission of imine moiety perhaps was not favorable for activity. This was further supported by the docking study of compound **4a** (Fig. 6, see also Fig S-10 of the suppl data). While a number of hydrophobic contacts with residues such as Phe214, Leu350$^{7.35}$ etc was observed in this case however the molecule **4a** unlike **3b** (**C-1**, Fig. 2) and **3i** (**C-2**, Fig. 3) missed the key aromatic pi-interactions that were essential for 5-HT_{2C}R agonism. Indeed, **4a** adopted a different binding pose perhaps due to the absence of imine moiety thereby decreasing its agonism potential. Similarly, the docking study of low active compound **3h** (see Fig S-5 in the suppl data) revealed (i) bad clashes between propyl side chain and the highly hydrophobic residues Leu209 and Val208^{EL2}, (ii) a steric clash between C-6 hydrogen of indole ring of **3h** and the residue Phe327 and (iii) a serious steric clash (generally referred as an ugly contact) between C-4 hydrogen of the indole ring and Val354. Nevertheless, EC_{50} values were determined for all the compounds (**3** and **4**) synthesized (see Table S-1, suppl data) and an overview of SAR (Structure-Activity-Relationship) observations noted from the current series of Schiff bases (**3**) is summarized in Fig. 7. In general, the methyl and benzyl group at indole nitrogen was beneficial for 5-HT_{2C}R agonism whereas other substituents like propargyl, allyl, ethyl and butyl or no substituent at this position decreased the activity. The presence of a long aliphatic chain such as pentyl or hexyl was not favorable at this position. The presence of a substituent at C-5 position of the indole ring was also appeared to be less favorable. Finally, the activity was influenced by the presence/absence of the imine moiety (e.g. compound **3** *vs* **4**). Having identified **3b** and **3i** as best active molecules

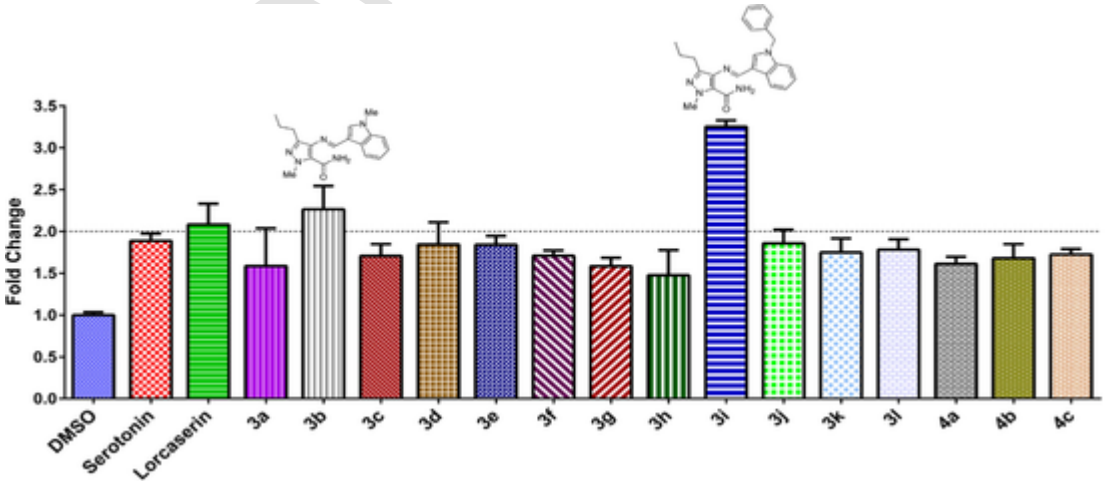

Fig. 5. Representative bar graph results of the primary screening of serotonin, Lorcaserin and test compounds (**3a-l** and **4a-c**) at 10 μM concentration against 5-HT_{2C} using the luciferase assay. The dashed line represents maximum effect of serotonin. The fold changes were plotted as mean ± SD. ****p < 0.0001, by one-way ANOVA Tukey's multiple comparisons test performed (n = 4) (see also one-way ANOVA in suppl data).

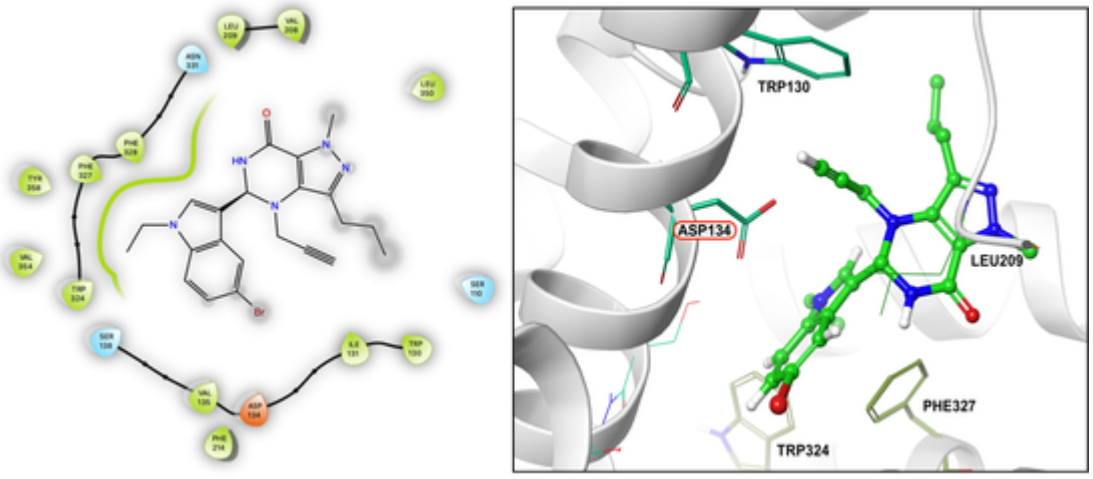

Fig. 6. The 2D and 3D interaction diagram between orthosteric binding site residues of $5HT_{2C}R$ and **4a.**

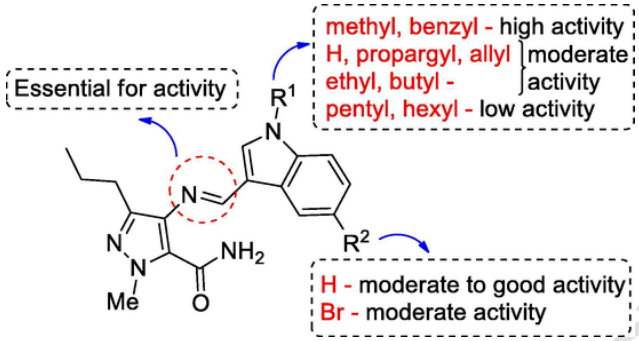

Fig. 7. Summary of SAR for $5\text{-}HT_{2C}R$ agonist activities of compound **3** (high activity > 2–3 fold response, moderate activity ≤ 2 fold response, low activity ~1.5–1.7 fold response).

against $5\text{-}HT_{2C}R$ it was became essential to determine their selectivity towards $5\text{-}HT_{2C}$ over $5\text{-}HT_{2A}$ and $5\text{-}HT_{2B}$. Accordingly, the concentration depend study was performed using these molecules along with serotonin and Lorcaserin against $5\text{-}HT_{2A}$ and $5\text{-}HT_{2B}$ receptors (Fig. 8) and EC_{50}, pEC_{50} and Emax values are summarized in Table 3. While both the compound **3b** and **3i** were found to be comparable with Lorcaserin from the viewpoint of EC_{50} value against $5\text{-}HT_{2C}$ (i.e. single digit nanomolar value) they showed better selectivity towards $5\text{-}HT_{2C}$ over 5- HT_{2A} (Table 4). For example, ~79 and ~24 fold selectivity was observed for compound **3b** and **3i** towards $5\text{-}HT_{2C}$ over $5\text{-}HT_{2A}$ respectively whereas that was ~14 fold in case of Lorcaserin. Similarly, ~21 and ~150 fold selectivity was observed for compound **3b** and **3i** towards $5\text{-}HT_{2C}$ over $5\text{-}HT_{2B}$ respectively compared to Lorcaserin's ~95 fold selectivity. Notably, with Emax = 222% the compound **3i** showed superior $5\text{-}HT_{2C}$ agonism over **3b** and Lorcaserin. The docking studies revealed that in spite of maintaining the pi-pi interaction with Phe340 of $5HT_{2A}R$ the compound **3b** (or **C-1**, Chart 1) participated in a less number of hydrophobic/van der Waals interactions (with residues Val156, Ile152, Trp151, Cys227, Leu228-229, Phe339 etc. and hydrophobic region of charged/polar residue Asp156, Ser159, Asn343 etc) compared to $5HT_{2C}R$ (see Fig S-6 and Table S-3 in Suppl data). Similarly, when docked into the $5HT_{2B}R$ the compound **3b** participated in the less number of interactions (with residues Leu209, Phe340, Trp337, Val136, Leu362, Val366 etc. and hydrophobic region of charged/polar residue Asp135, Glu363, and Ser139) (see Fig S-7 and Table S-3 in Suppl data).

A similar trend was also observed in case of compound **3i** (or **C-2**, Chart 1) (see Fig S-8 and S-9 and Table S-3 in Suppl data) accounting its selectivity towards $5\text{-}HT_{2C}$ over $5\text{-}HT_{2A}$ and $5\text{-}HT_{2B}$. It is worthy to mention that though **3b** and **3i** (**C-1** and **C-2**, Chart 1) were expected to show a better affinity for $5\text{-}HT_{2C}$ than Lorcaserin, (as predicted by the *in silico* studies) this difference did not appear as dramatic in the *in vitro* assay (Table 3). Similarly, the higher affinity of **3i** (or **C-2**) over **3b** (or **C-1**) as predicted *in silico* (Chart 1) was also not reflected by their EC_{50} values (Table 3). However, it is known that the binding affinities predicted *via* the molecular docking (a static system) do not always corroborate well the biological response (a dynamic system) observed in the *in vitro* assays [42].

Till this stage of the study our SAR focus was primarily on the indole moiety of compound **3** whereas the pyrazole part largely remained unexplored. However, to gain some insight regarding the role of substituents present on the pyrazole ring we performed docking studies using the $5HT_{2C}$ and the designed analogues of **3b** i.e. compound **3m**, **3n** and **3o** where the substituents present on the pyrazole ring was varied systematically (see Fig. S-11 in Suppl data). The outcome of *in silico* studies indicated inferior docking scores for **3m** (-6.8 kcal/mol), **3n** (−6.6 kcal/mol) and **3o** (−6.3 kcal/mol) compared to **3b** (or **C-1** with −9.4 kcal/mol, Chart 1). A gradual decrease in docking score was also noted with the sequential removal of amide, *n*-propyl and *N*-methyl substituent from the pyrazole ring. While the role of indole ring was understandable from the *in silico* studies however to gain further evidence the compound **3p** [or (*E*)-4-((4-hydroxybenzylidene)amino)-1-methyl-3-propyl-1*H*-pyrazole-5-carboxamide prepared *via* the reaction of **1a** with 4-hydroxybenzaldehyde, see the experimental section] where the indole ring was replaced an aryl moiety was evaluated against $5\text{-}HT_{2C}$ for agonist activity using the luciferase assay when the compound showed low activity (1.6 fold response at 10 μM).

Due to their structural relevance to the known indole based PAM of $5\text{-}HT_{2C}$ receptor **A** (Fig. 1) the PAM activity of compound **3b** and **3i** was assessed by using a NFAT-RE luciferase assay [41]. The test compounds were added at a concentration of 10 μM in quadruplicate followed by addition of serotonin at 10 μM concentration to the assay plate. The results presented in Fig. 9 suggested that like Lorcaserin none of **3i** or **3b** showed $5HT_{2C}$-PAM activity though some synergistic effects were noted as a result of serotonin addition.

Next, following the routine strategy of Med Chem we conducted some initial assessment about ADME (absorption, distribution, metabolism, and excretion) or pharmacokinetic properties of compound **3b** and **3i** along with Lorcaserin. Thus, the computational ADME prediction of these compounds was carried out using Swiss ADME web-tool [43] (see experimental section) and results are summarized in Table 5 (among the various descriptors only notable one are listed in the table). The desirable ADME was predicted for both the compound **3b** and **3i** including the high GI absorption. Moreover, none of these compounds

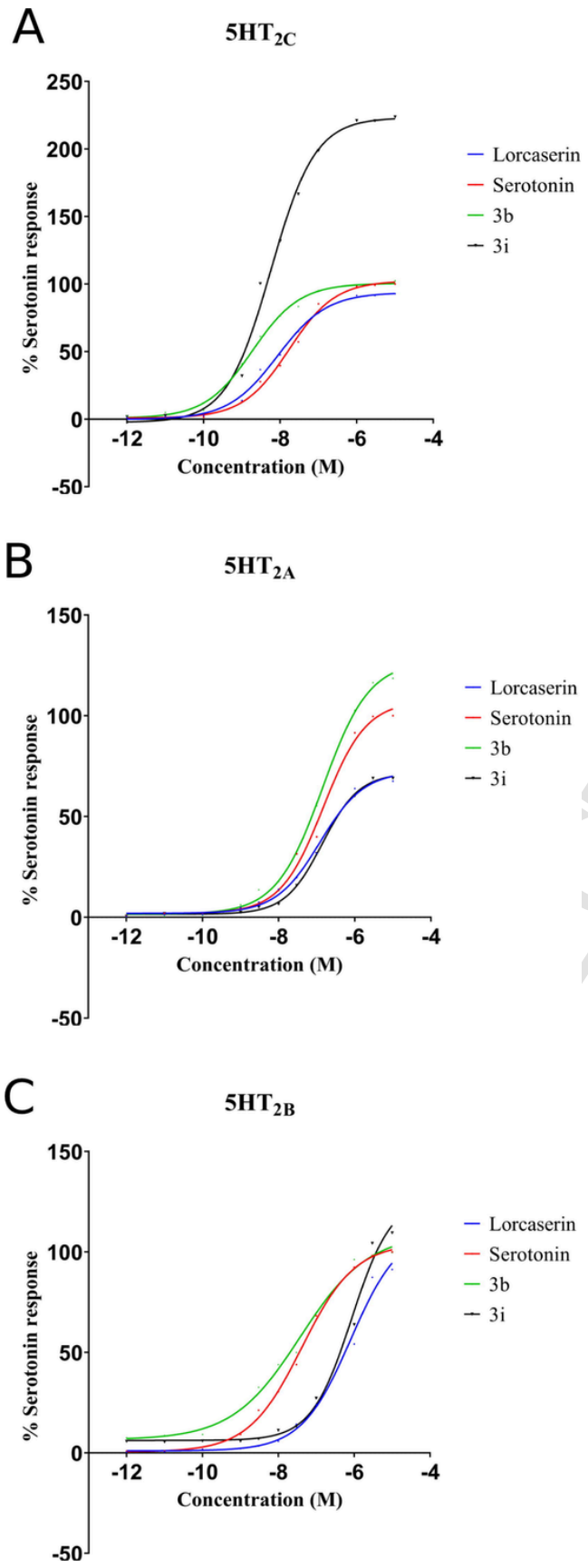

Fig. 8. The concenration response curves for serotonin, Lorcaserin, **3b** and **3i** against (A) 5-HT_{2C} (B), 5-HT_{2A} and (C) 5-HT_{2B} receptors generated using transiently transfected HEK293T cells with NFAT-RE luciferase. The curves were plotted as mean ± SEM (N = 3) (for standard deviations, see Table 3).

showed violation of Lipinski or Veber rule that predicted favorable drug like properties for **3b** and **3i**.

In order to gain some preliminary idea regarding the effect of **3b** and **3i** on 5-HT_{2C} in an *in vivo* system (and encouraged by the desirable ADME predictions *in silico*) we measured the locomotor activity of these compounds along with Lorcaserin in the zebrafish (Danio rerio) larvae model. Notably, the 5-HT_{2C} receptor agonist such as CP809101 has been reported to reduce the locomotor activity in C57BL/6 mice [44a]. Moreover, activation of 5-HT_{2C} receptors by Ro 60-0175 (a 5-HT_{2C} agonist) reduced the locomotor and rewarding effects of nicotine in rats [44b] whereas Lorcaserin at 10 μM reduced the velocity significantly in zebrafish along with reduction in seizure frequency and/or severity at higher doses [44c]. Notably, a zebrafish model of DIO that shared common pathophysiological pathways with mammalian obesity was established in 2010 with the goal of using the model to identify putative pharmacological targets and to test novel drugs for the treatment of human obesity [44d]. Further, due to the similarities to mammalian 5-HT_{2C}R genes the zebrafish has been suggest to use for the study of 5-HT_{2C}R function in behavior, development and drug discovery [44e]. In the current study, carried out following a reported method [44f] the 6 days post-fertilization (6 dpf) zebrafish larvae were exposed to the test compounds i.e. 10 and 30 μM of **3b**, 10 μM of **3i** and 10 μM of Lorcaserin. The larvae used per concentration was 48. The locomotor activity was measured *via* the total distance (mm) moved by larvae in 10 min using the ZebraLab software (Fig. 10). While the compound **3b** did not show any significant effects even at 30 μM the effect of **3i** was found to be comparable to Lorcaserin. The lack of activity of **3b** was initially thought to be due to its lower ability to cross the blood brain barrier (BBB) thereby low interactions with the $5HT_{2C}$ in the brain. However, the BBB penetration score (0.064, 0.084 and 0.115 of **3b**, **3i** and Lorcaserin, respectively) obtained *via* BBB Predictor tool [45a] indicated that the score of **3b** (though lower than **3i** and Lorcaserin) was higher than the BBB threshold of 0.02 for poor or good permeability through blood brain barrier. Moreover, the logP and logS values for **3b** were

similar to those of Lorcaserin (Table 5) possessing a good BBB permeability. We then focused on evaluation of metabolic stability of **3b** and **3i** *in vitro* in the presence of mouse liver microsomes (MLM) (Fig. 11). The liver microsomes (the subcellular particles derived from the endoplasmic reticulum of hepatic cells) are known to be a rich source of drug metabolizing enzymes, including cytochrome *P*-450. Being a widely used initial cell-based model system MLM can correlate well with the liver microsomal stability in other species including human [45b]. At a concentration of 5 μM the compound **3b** showed relatively much lower stability after 60 min [the mean % of **3b** remaining after 60 min compared to 0 min ~4.85; half-life ($t_{1/2}$, min) ~13.56 and intrinsic clearance (CL_{int}, μL/min/mg) ~215.30] than **3i** [the mean % of **3i** remaining after 60 min compared to 0 min ~36.47; half-life ($t_{1/2}$, min) ~90.16 and intrinsic clearance (CL_{int}, μL/min/mg) ~34.30] and Lorcaserin (the mean % remaining after 60 min compared to 0 min ~59.96). Based on the fact that *N*-demethylation is a common metabolic path for *N*-methyl indole drugs [45c] the low MLM stability of **3b** could be accounted by the *N*-demethylation of its indole ring that was not possible in case of **3i** thereby accounting its higher stability. On the other hand, *N*-demethylation of the pyrazole ring in case of **3i** (and in case of **3b** also) was responsible for its lower stability than Lorcaserin. Nevertheless, the MLM stability data suggests that **3b** and **3i** may possess relatively better stability than the common Schiff bases (that are known to display pronounced hydrolytic lability) [45d] due to the intramolecular H-bond involving the imine hydrogen and the proximate –$CONH_2$ moiety thereby forming a stable 6-membered chelating ring. The existence of such type of intramolecular H-bond in this class of

Table 3
$EC_{50,}$ Emax and pEC_{50} values of **3b**, **3i**, serotonin and Lorcaserin against 5-HT_2 receptors, values are normalized by the 5-HT response (N = 3).

	$5HT_{2C}$			$5HT_{2A}$			$5HT_{2B}$		
Compound	EC_{50} (nM)	Emax (%)	pEC_{50}	EC_{50} (nM)	Emax (%)	pEC_{50}	EC_{50} (nM)	Emax (%)	pEC_{50}
Serotonin	17.1 ± 4.8	100	7.76 ± 0.07	148.8 ± 8.1	100	6.82 ± 0.02	41.5 ± 3.1	100	7.38 ± 0.03
Lorcaserin	8.5 ± 0.5	92.5	8.07 ± 0.02	121 ± 7.2	66.2	6.91 ± 0.02	804.1 ± 65	106.62867	6.09 ± 0.03
3b	1.8 ± 0.4	98.2	8.72 ± 0.08	142.8 ± 23	119.3	6.84 ± 0.07	37.8 ± 29	98.4869	7.42 ± 0.53
3i	5.7 ± 0.1	222	8.24 ± 0.20	139.4 ± 17	65.7	6.85 ± 0.05	852 ± 34	117.105	6.06 ± 0.01

Table 4
Selectivity of **3b**, **3i** and Lorcaserin (values are normalized by the 5-HT response (N = 3)).

Compounds	Fold selectivity	
	5-HT_{2A}/5-HT_{2C}	5-HT_{2B}/5-HT_{2C}
Lorcaserin	14.24	95
3b	79.33	21
3i	24.46	150

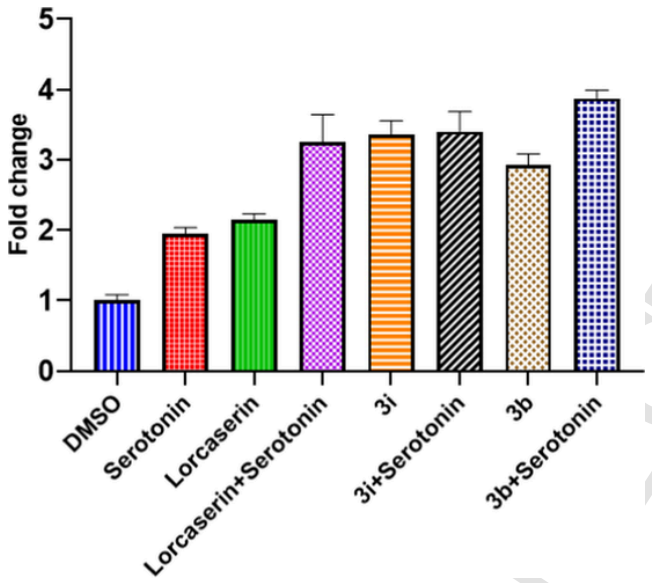

Fig. 9. Evaluation of compounds on 5-HT_{2C} for PAM activity using NFAT-RE luciferase assay. The fold changes were plotted as mean ± SD (n = 4).

Table 5
Computational ADME prediction of **3b**, **3i** and Lorcaserin.

Properties	Molecules		
(i) Physicochemical	**3b**	**3i**	Lorcaseirn
Molecular Weight (g/mol)	323.39	399.49	195.69
Consensus Log P[a]	2.22	3.51	2.75
Log S (ESOL)[b]	−3.21 (soluble)	−4.62 (moderately soluble)	−3.12 (soluble)
(ii) Pharmacokinetics			
GI[c] absorption	High	High	High
(iii) Drug likeness			
Lipinski rule	NV	NV	NV
Veber rule	NV	NV	NV

NV: No violation.
[a] Log P: Lipophilicity.
[b] Log S (ESOL): water solubility, calculated by ESOL method which is a Quantitative Structure-Property Relationship (QSPR) based model.
[c] GI: Gastrointestinal.

Chart 1
Docking score of molecules with $5HT_{2C}$R.

Molecules	Docking score (Kcal/mol)
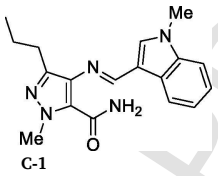 **C-1**	−9.4
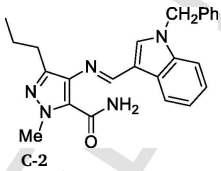 **C-2**	−10.7
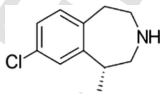 **L**	−7.0
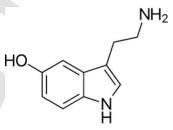 **S**	−6.6

***L** and **S** are known/reference compounds

compounds (e.g. **3p**) has been reported previously [45e] (see suppl data). Overall, based on *in silico*, *in vitro* and *in vivo* data and being a new chemotype these compounds especially **3i** could be considered for further profiling.

3. Conclusion

In conclusion, a series of indole based novel Schiff bases was designed as potential agonists of 5-HT_{2C} receptor and was evaluated *in silico via* docking studies. These compounds were accessed conveniently *via* condensation of an appropriate pyrazole based primary amine with the corresponding indole-3-aldehyde in the presence of a heterogeneous catalyst i.e. Amberlyst-15 under ultrasound irradiation at ambient temperature. A number of target Schiff bases were obtained in good yields (77–87%) under mild conditions within 1 h. Notably, the methodology afforded the corresponding cyclized products i.e. pyrazolo[4,3-*d*]pyrimidin-7(4*H*)-one derivatives when the primary amine was replaced by a secondary amine. Several Schiff bases showed agonist activity when tested against human 5-HT_{2C} using luciferase assay in HEK293T cells *in vitro*. The SAR (Structure-Activity-Relationship) studies suggested that the imine moiety was more favorable over its cyclic form i.e. the pyrazolopyrimidinone ring. Moreover, the presence of methyl or benzyl moiety at the indole nitrogen was found to be beneficial in case of Schiff bases. The Schiff bases **3b** (EC_{50} = 1.8 nM) and **3i** (EC_{50} = 5.7 nM) were identified as the most active compounds and were comparable with Lorcaserin (EC_{50} = 8.5 nM). Also like Lorcaserin, none of these compounds were found to be PAM of 5-HT_{2C}.

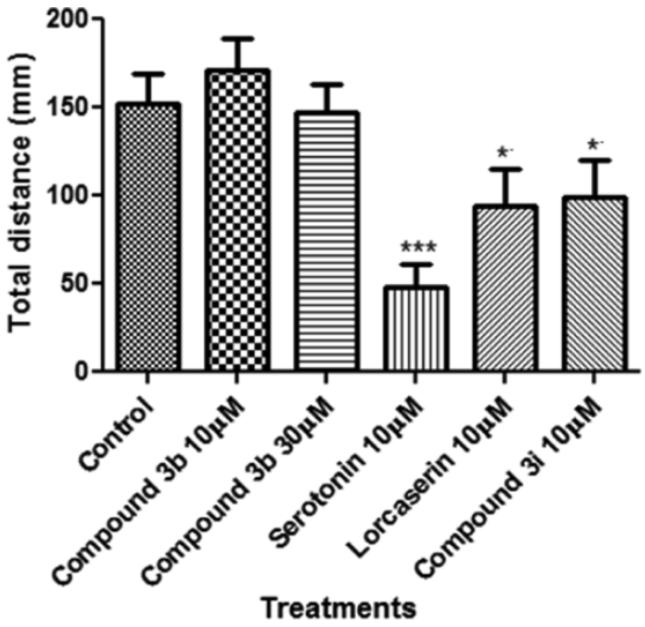

Fig. 10. The locomotor activity of **3b**, **3i** and Lorcaserien in the zebrafish (Danio rerio) larvae model (N = 3). The graph is plotted with mean ± standard error of the mean and the statistically significance calculated using graph pad prism software is indicated with asterisks (*P < 0.05; **P < 0.01; ***P < 0.001).

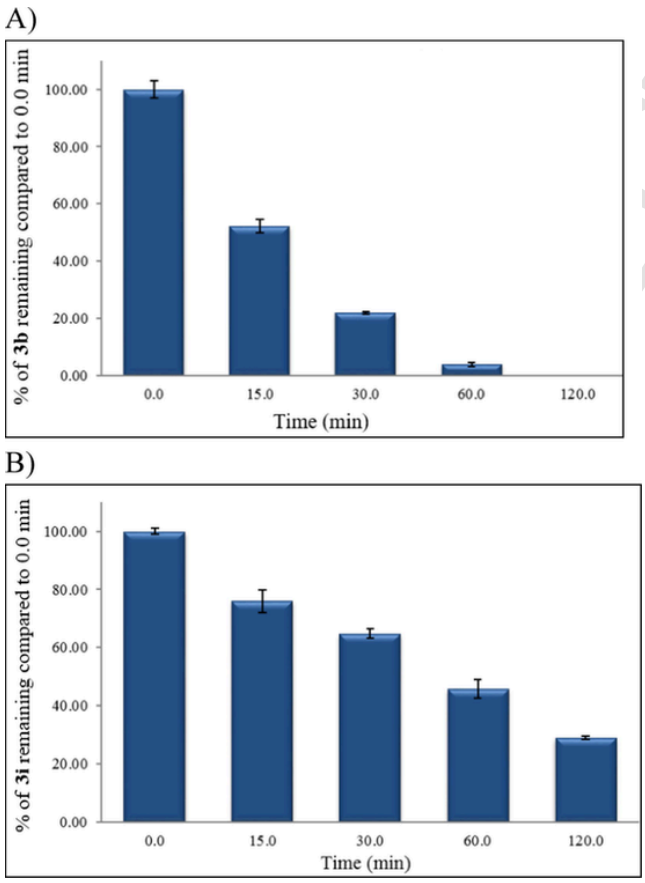

Fig. 11. Metabolic stability of (A) compound **3b** and (B) **3i** in mouse liver microsomes.

With ~24 and ~150 fold selectivity towards 5-HT_{2C} over 5-HT_{2A} and 5-HT_{2B} respectively the compound **3i** that reduced locomotor activity in zebrafish (Danio rerio) larvae model emerged as a promising hit molecule for further development. Overall, the current research not only demonstrated the utility of heterogeneous catalysis under ultrasound for the direct access of densely substituted novel indole derivatives but also presented a new framework for the design and identification of promising and selective 5-HT_{2C}R agonists thereby potential anti-obesity agents.

4. Experimental section

4.1. Chemistry

4.1.1. General methods

Unless stated otherwise, reactions were performed under nitrogen atmosphere using oven dried glassware. Reactions were monitored by thin layer chromatography (TLC) on silica gel plates (60 F254), visualizing with ultraviolet light or iodine spray. Flash chromatography was performed on silica gel (230–400 mesh) using distilled hexane and EtOAc. ^{1}H and ^{13}C NMR spectra were recorded in DMSO-d_6 solution by using a 400 and 100 MHz spectrometer. Proton chemical shifts (δ) are relative to tetramethylsilane (TMS, δ = 0.00) as internal standard and expressed in ppm. Spin multiplicities are given as s (singlet), d (doublet), dd (doublet of doublet), td (triplet of doublet), t (triplet) and m (multiplet) as well as bs (broad singlet). Coupling constants (*J*) are given in hertz. Melting points were determined using melting point apparatus and are uncorrected. MS spectra were obtained on Agilent 6430 series Triple Quard LC-MS/MS spectrometer. Chromatographic purity by HPLC (Agilent 1200 series ChemStation software) was determined by using area normalization method and the condition Specified in each case: column, mobile phase (range used), flow rate, diluent, detection wavelength, and retention times. All the ultrasound assisted reactions were carried out using a laboratory ultrasonic bath SONOREX SUPER RK 510H model producing irradiation of 35 kHz.

4.1.2. General procedure for the preparation of compound *3* and *4*

To a stirred solution of amine **1** (1.0 mmol) in acetonitrile (5 mL), amberlyst-15 (10% w/w) was added and the reaction mixture mixture was allowed to stirr for few minutes. Then the corresponding carbonyl compound **2** (1.1 mmol) was added and the reaction mixture was irradiated with ultrasound (35 KHz) continuously at room temperature (25–30 °C) for 1 h. The temperature of the bath was maintained by adding cold water time to time in case any increase in bath temperature was observed as a result of prolonged irradiation. The progress of the reaction is monitored by TLC and after the completion of the reaction acetonitrile was evaporated by rotary evaporator. The crude residue was purified by column chromatography on silica gel using 10% EtOAc in hexane to afford the desired product. All the compounds (**3a–l, 4a-c**) prepared were characterized by MS, NMR spectra and purity was determined by HPLC method.

4.1.3. (E)-4-[{(1H-Indol-3-yl)methylene}amino]-1-methyl-3-propyl-1H-pyrazole-5-carboxamide (*3a*)

White solid (77% yield); mp: 187–189 °C; R_f = 0.22 (40% EtOAc/*n*-hexane); ^{1}H NMR (400 MHz, DMSO-d_6) δ: 11.90 (bs, 1H, indole NH, D_2O exchangeable), 8.71 (s, 1H, -N = CH–), 8.23 (bs, 1H, NH, D_2O exchangeable), 8.15 (d, *J* = 7.6 Hz, 1H, ArH), 8.09 (s, 1H, indole (C-2) H), 7.75 (bs, 1H, NH, D_2O exchangeable), 7.51 (d, *J* = 8.0 Hz, 1H, ArH), 7.25 (t, *J* = 7.6 Hz, 1H, ArH), 7.19 (t, *J* = 7.6 Hz, 1H, ArH), 4.04 (s, 3H, NCH_3), 2.67 (t, *J* = 7.6 Hz, 2H, CH_2), 1.72–1.60 (m, 2H, $MeCH_2$), 0.93 (t, *J* = 7.6 Hz, 3H, CH_3); ^{13}C NMR (100 MHz, DMSO-d_6) δ: 161.1 (C═O), 157.2, 140.0, 137.4, 134.6, 133.4, 126.9, 124.3, 123.1, 121.4, 120.8, 114.7, 112.4, 39.3 (NMe), 28.3 (CH_2), 21.3 (CH_2), 14.0 (Me); HPLC: 95.2%, Column: X-Bridge C-18 150*4.6 mm 5 μm,

mobile phase A: 5 mM Ammonium acetate in water, mobile phase B: CH_3CN, (gradient) T/B% : 0/10, 23/90, 30/90, 31/10, 35/10; flow rate: 1 mL/min, Diluent: CH_3CN: water (80:20), UV: 220.0 nm, retention time 12.6 min; MS (ES mass): *m/z* 310.1 (M + 1, 100%).

*4.1.4. (E)-1-Methyl-4-[{(1-methyl-1H-indol-3-yl)methylene}amino]-3-propyl-1H-pyrazole-5-carboxamide **(3b)***

White solid (87% yield); mp: 170–172 °C; R_f = 0.27 (40% EtOAc/*n*-hexane); ^{1}H NMR (400 MHz, DMSO-d_6) δ: 8.67 (s, 1H, -N = CH–), 8.19 (bs, 1H, NH, D_2O exchangeable), 8.15 (d, *J* = 7.6 Hz, 1H, ArH), 8.08 (s, 1H, indole (C-2) H), 7.75 (bs, 1H, NH, D_2O exchangeable), 7.58 (d, *J* = 8.0 Hz, 1H, ArH), 7.33(t, *J* = 7.2 Hz, 1H, ArH), 7.24 (t, *J* = 7.2 Hz,1H, ArH), 4.04 (s, 3H, NCH_3), 3.88 (s, 3H, NCH_3), 2.67 (t, *J* = 7.6 Hz, 2H, CH_2), 1.72–1.59 (m, 2H, $MeCH_2$), 0.92 (t, *J* = 7.6 Hz, 3H, CH_3); ^{13}C NMR (100 MHz, DMSO-d_6) δ: 161.1 (C═O), 156.6, 140.0, 137.9, 137.8, 133.3, 126.9, 124.7, 123.1, 121.7, 120.8, 113.6, 110.8, 39.3 (NMe), 33.0 (NMe), 28.3 (CH_2), 21.4 (CH_2), 14.0 (Me); HPLC: 96.9%, Column: X-Bridge C-18 150*4.6 mm 5 µm, mobile phase A: 5 mM Ammonium acetate in water, mobile phase B: CH_3CN, (gradient) T/B% : 0/5, 20/90, 30/90, 31/5, 35/5; flow rate: 1 mL/min, Diluent: CH_3CN: water (80:20), UV: 220.0 nm, retention time 13.9 min; MS (ES mass): *m/z* 324.1 (M + 1, 100%).

*4.1.5. (E)-4-[{(1-Ethyl-1H-indol-3-yl)methylene}amino]-1-methyl-3-propyl-1H-pyrazole-5-carboxamide **(3c)***

White solid (85% yield); mp: 96–98 °C; R_f = 0.32 (40% EtOAc/*n*-hexane); ^{1}H NMR (400 MHz, DMSO-d_6) δ: 8.68 (s, 1H, -N = CH–), 8.19 (bs, 1H, NH, D_2O exchangeable), 8.17 (d, *J* = 7.6 Hz, 1H, ArH), 8.15 (s, 1H, indole (C-2) H), 7.75 (bs, 1H, NH, D_2O exchangeable), 7.62 (d, *J* = 8.0 Hz, 1H, ArH), 7.34–7.28 (m, 1H, ArH), 7.25–7.20 (m, 1H, ArH), 4.29 (q, *J* = 7.2 Hz, 2H, NCH_2), 4.07 (s, 3H, NCH_3), 2.67 (t, *J* = 7.6 Hz, 2H, propyl-CH_2), 1.71–1.61 (m, 2H, propyl-CH_2), 1.44 (t, *J* = 7.2 Hz, 3H, CH_3), 0.95 (t, *J* = 7.6 Hz, 3H, CH_3); ^{13}C NMR (100 MHz, DMSO-d_6) δ: 161.1 (C═O), 156.6, 140.0, 137.0, 136.4, 133.3, 126.9, 124.9, 123.1, 121.7, 121.0, 113.8, 110.8, 40.9 (NCH_2), 39.3 (NMe), 28.3 (CH_2), 21.4 (CH_2), 15.1 (Me), 14.0 (Me); HPLC: 94.2%, Column: X-Bridge C-18 150*4.6 mm 5 µm, mobile phase A: 5 mM Ammonium acetate in water, mobile phase B: CH_3CN, (gradient) T/B% : 0/10, 23/90, 30/90, 31/10, 35/10; flow rate: 1 mL/min, Diluent: CH_3CN: water (80:20), UV: 220.0 nm, retention time 15.7 min; MS (ES mass): *m/z* 338.2 (M + 1, 100%).

*4.1.6. (E)-1-Methyl-4-[{(1-(prop-2-yn-1-yl)-1H-indol-3-yl)methylene}amino]-3-propyl-1H-pyrazole-5-carboxamide **(3d)***

Pale Yellow solid (85% yield); mp: 159–161 °C; R_f = 0.38 (40% EtOAc/*n*-hexane); ^{1}H NMR (400 MHz, DMSO-d_6) δ: 8.72 (s, 1H, -N = CH–), 8.19 (d, *J* = 8.0 Hz, 1H, ArH), 8.17 (s, 1H, indole (C-2) H), 8.14 (bs, 1H, NH, D_2O exchangeable), 7.77 (bs, 1H, NH, D_2O exchangeable), 7.66 (d, *J* = 8.4 Hz, 1H, ArH), 7.37–7.33 (m, 1H, ArH), 7.29–7.24 (m, 1H, ArH), 5.22 (d, *J* = 2.8 Hz, 2H, NCH_2), 4.04 (s, 3H, NCH_3), 3.53 (t, *J* = 2.8 Hz, 1H, HC≡C), 2.67 (t, *J* = 7.6 Hz, 2H, CH_2), 1.75–1.58 (m, 2H, $MeCH_2$), 0.93 (t, *J* = 7.6 Hz, 3H, CH_3); ^{13}C NMR (100 MHz, DMSO-d_6) δ: 161.1 (C═O), 156.7, 140.1, 136.8, 136.3, 133.1, 127.0, 124.9, 123.4, 122.0, 121.1, 114.5, 111.1, 78.4 (-C≡), 76.5 (HC≡), 39.3 (NMe), 35.7 (NCH_2), 28.3 (CH_2), 21.3 (CH_2), 14.0 (Me); HPLC: 98.9%, Column: Eclipse XDB 150*4.6 µm, mobile phase A: 5 mM Ammonium acetate in water, mobile phase B: CH_3CN, (gradient) T/B%: 0/5, 20/90, 30/90, 31/5, 35/5; flow rate: 1 mL/min, Diluent: CH_3CN: water (80:20), UV: 220.0 nm, retention time 13.9 min; MS (ES mass): *m/z* 348.2 (M + 1, 100%).

*4.1.7. (E)-4-[{(1-Allyl-1H-indol-3-yl)methylene}amino]-1-methyl-3-propyl-1H-pyrazole-5-carboxamide **(3e)***

Pale Yellow solid (82% yield); mp: 112–114 °C; R_f = 0.41 (40% EtOAc/*n*-hexane); ^{1}H NMR (400 MHz, DMSO-d_6) δ: 8.70 (s, 1H, -N = CH–), 8.20–8.16 (m, 2H, ArH, NH, D_2O exchangeable), 8.10 (s, 1H, indole (C-2) H), 7.75 (bs, 1H, NH, D_2O exchangeable), 7.57 (d, *J* = 8.0 Hz, 1H, ArH), 7.35–7.27 (m, 1H, ArH), 7.27–7.19 (m, 1H, ArH), 6.10–6.00 (m, 1H, Allyl CH), 5.29–5.10 (m, 2H, =CH_2), 4.92 (d, *J* = 5.6 Hz, 2H, NCH_2), 4.05 (s, 3H, NCH_3), 2.67 (t, *J* = 7.6 Hz, 2H, CH_2), 1.74–1.59 (m, 2H, $MeCH_2$), 0.92 (t, *J* = 7.6 Hz, 3H, CH_3); ^{13}C NMR (100 MHz, DMSO-d_6) δ: 161.1 (C═O), 156.6, 140.0, 137.2, 136.9, 133.5, 133.2, 126.9, 124.8, 123.1, 121.7, 121.0, 117.7, 114.1, 111.1, 48.5 (NCH_2), 39.3 (NMe), 28.3 (CH_2), 21.3 (CH_2), 14.0 (Me); HPLC: 95.4%, Column: X-Bridge C-18 150*4.6 mm 5 µm, mobile phase A: 5 mM Ammonium acetate in water, mobile phase B: CH_3CN, (gradient) T/B% : 0/5, 20/90, 30/90, 31/5, 35/5; flow rate: 1 mL/min, diluent: CH_3CN: water (80:20), UV: 225.0 nm, retention time 15.2 min; MS (ES mass): *m/z* 350.2 (M + 1, 100%).

*4.1.8. (E)-4-[{(1-Butyl-1H-indol-3-yl)methylene}amino]-1-methyl-3-propyl-1H-pyrazole-5-carboxamide **(3f)***

White solid (87% yield); mp: 128–130 °C; R_f = 0.48 (40% EtOAc/*n*-hexane); ^{1}H NMR (400 MHz, DMSO-d_6) δ: 8.67 (s, 1H, -N = CH–), 8.20 (bs, 1H, NH, D_2O exchangeable), 8.17 (d, *J* = 7.6 Hz, 1H, ArH), 8.12 (s, 1H, indole (C-2) H), 7.74 (bs, 1H, NH, D_2O exchangeable), 7.62 (d, *J* = 8.0 Hz, 1H, ArH), 7.33–7.27 (m, 1H, ArH), 7.24–7.20 (m, 1H, ArH), 4.25 (t, *J* = 7.2 Hz, 2H, NCH_2), 4.04 (s, 3H, NCH_3), 2.67 (t, *J* = 7.6 Hz, 2H, propyl-CH_2), 1.87–1.74 (m, 2H, CH_2), 1.71–1.61 (m, 2H, propyl-CH_2), 1.34–1.24 (m, 2H, CH_2), 0.95–0.88 (m, 6H, $2CH_3$); ^{13}C NMR (100 MHz, DMSO-d_6) δ: 161.1 (C═O), 156.6, 140.0, 137.3, 136.9, 133.3, 126.9, 124.8, 123.0, 121.6, 121.0, 113.8, 110.9, 45.7 (NCH_2), 39.3 (NMe), 31.6 (CH_2), 28.3 (CH_2), 21.4 (CH_2), 19.4 (CH_2), 14.0 (Me), 13.5 (Me); HPLC: 97.1%, Column: X-Bridge C-18 150*4.6 mm 5 µm, mobile phase A: 5 mM Ammonium acetate in water, mobile phase B: CH_3CN, (gradient) T/B% : 0/5, 20/90, 30/90, 31/5, 35/5; flow rate: 1 mL/min, Diluent: CH_3CN: water (80:20), UV: 225.0 nm, retention time 17.1 min; MS (ES mass): *m/z* 366.2 (M + 1, 100%).

*4.1.9. (E)-1-Methyl-4-[{(1-pentyl-1H-indol-3-yl)methylene}amino]-3-propyl-1H-pyrazole-5-carboxamide **(3g)***

White solid (84% yield); mp: 120–122 °C; R_f = 0.55 (40% EtOAc/*n*-hexane); ^{1}H NMR (400 MHz, DMSO-d_6) δ: 8.67 (s, 1H, -N = CH–), 8.21 (bs, 1H, NH, D_2O exchangeable), 8.17 (d, *J* = 7.6 Hz, 1H, ArH), 8.13 (s, 1H, indole (C-2) H), 7.76 (bs, 1H, NH, D_2O exchangeable), 7.61 (d, *J* = 8.0 Hz, 1H, ArH), 7.32–7.27 (m, 1H, ArH), 7.24–7.20 (m, 1H, ArH), 4.24 (t, *J* = 7.2 Hz, 2H, NCH_2), 4.04 (s, 3H, NCH_3), 2.67 (t, *J* = 7.6 Hz, 2H, propyl-CH_2), 1.87–1.74 (m, 2H, CH_2), 1.72–1.60 (m, 2H, propyl-CH_2), 1.37–1.19 (m, 4H, $2CH_2$), 0.93 (t, *J* = 7.6 Hz, 3H, propyl-CH_3), 0.84 (t, *J* = 7.2 Hz, 3H, pentyl-CH_3); ^{13}C NMR (100 MHz, DMSO-d_6) δ: 161.1 (C═O), 156.6, 140.0, 137.3, 137.0, 133.3, 126.9, 124.8, 123.1, 121.6, 121.0, 113.8, 110.9, 46.0 (NCH_2), 39.3 (NMe), 29.2 (CH_2), 28.4 (CH_2), 28.3 (CH_2), 21.7 (CH_2), 21.4 (CH_2), 14.0 (Me), 13.8 (Me); HPLC: 96.9%, Column: X-Bridge C-18 150*4.6 mm 5 µm, mobile phase A: 5 mM Ammonium acetate in water, mobile phase B: CH_3CN, (gradient) T/B% : 0/10, 23/90, 30/90, 31/10, 35/10; flow rate: 1 mL/min, Diluent: CH_3CN: water (80:20), UV: 220.0 nm, retention time 19.8 min; MS (ES mass): *m/z* 380.2 (M + 1, 100%).

*4.1.10. (E)-4-[{(1-Hexyl-1H-indol-3-yl)methylene}amino]-1-methyl-3-propyl-1H-pyrazole-5-carboxamide **(3h)***

White solid (86% yield); mp: 101–103 °C; R_f = 0.60 (40% EtOAc/*n*-hexane); ^{1}H NMR (400 MHz, DMSO-d_6) δ: 8.68 (s, 1H, -N = CH–), 8.20 (bs, 1H, NH, D_2O exchangeable), 8.17 (d, *J* = 7.6 Hz, 1H, ArH), 8.12 (s, 1H, indole (C-2) H), 7.75 (bs, 1H, NH, D_2O exchangeable), 7.61 (d, *J* = 8.0 Hz, 1H, ArH), 7.33–7.27 (m, 1H, ArH), 7.25–7.19 (m, 1H, ArH), 4.24 (t, *J* = 7.2 Hz, 2H, NCH_2), 4.04 (s, 3H, NCH_3), 2.67 (t, *J* = 7.6 Hz, 2H, propyl-CH_2), 1.86–1.74 (m, 2H, CH_2), 1.72–1.60 (m, 2H, propyl-CH_2), 1.31–1.22 (m, 6H, $3CH_2$), 0.93 (t, *J* = 7.6 Hz, 3H,

propyl-CH_3), 0.84 (t, J = 7.2 Hz, 3H, pentyl-CH_3); ^{13}C NMR (100 MHz, DMSO-d_6) δ: 161.1 (C═O), 156.6, 140.0, 137.2, 136.9, 133.3, 126.9, 124.8, 123.0, 121.6, 121.0, 113.8, 110.9, 46.0 (NCH_2), 39.3 (NMe), 30.7 (CH_2), 29.4 (CH_2), 28.3 (CH_2), 25.8 (CH_2), 21.9 (CH_2), 21.3 (CH_2), 13.9 (Me), 13.8 (Me); HPLC: 97.9%, Column: X-Bridge C-18 150*4.6 mm 5 μm, mobile phase A: 5 mM Ammonium acetate in water, mobile phase B: CH_3CN, (gradient) T/B% : 0/5, 20/90, 30/90, 31/5, 35/5; flow rate: 1 mL/min, diluent: CH_3CN: water (80:20), UV: 225.0 nm, retention time 19.4 min; MS (ES mass): *m/z* 394.2 (M+1, 100%).

*4.1.11. (E)-4-[{(1-Benzyl-1H-indol-3-yl)methylene}amino]-1-methyl-3-propyl-1H-pyrazole-5-carboxamide **(3i)***

White solid (87% yield); mp: 138–140 °C; R_f = 0.47 (40% EtOAc/*n*-hexane); ^{1}H NMR (400 MHz, DMSO-d_6) δ: 8.72 (s, 1H, -N = CH–), 8.26 (s, 1H, indole (C-2) H), 8.22–8.16 (m, 2H, ArH, NH, D_2O exchangeable), 7.77 (bs, NH, D_2O exchangeable), 7.60 (d, J = 8.0 Hz, 1H, ArH), 7.37–7.19 (m, 7H, ArH), 5.52 (s, 2H, NCH_2), 4.05 (s, 3H, NCH_3), 2.67 (t, J = 7.6 Hz, 2H, CH_2), 1.74–1.61 (m, 2H, $MeCH_2$), 0.93 (t, J = 7.6 Hz, 3H, CH_3); ^{13}C NMR (100 MHz, DMSO-d_6) δ: 161.1 (C═O), 156.6, 140.1, 137.2, 137.2, 133.2, 128.7 (2C), 127.7, 127.3 (2C), 127.0, 125.0, 123.3, 121.8, 121.1, 114.3, 111.3, 49.6 (NCH_2), 39.3 (NMe), 28.3 (CH_2), 21.4 (CH_2), 14.0 (Me); HPLC: 96.0%, Column: X-Bridge C-18 150*4.6 mm 5 μm, mobile phase A: 5 mM Ammonium acetate in water, mobile phase B: CH_3CN, (gradient) T/B% : 0/5, 20/90, 30/90, 31/5, 35/5; flow rate: 1 mL/min, Diluent: CH_3CN: water (80:20), UV: 220.0 nm, retention time 16.7 min; MS (ES mass): *m/z* 400.2 (M+1, 100%).

*4.1.12. (E)-4-[{(5-Bromo-1H-indol-3-yl)methylene}amino]-1-methyl-3-propyl-1H-pyrazole-5-carboxamide **(3j)***

White solid (77% yield); mp: 201–203 °C; R_f = 0.21 (40% EtOAc/*n*-hexane); ^{1}H NMR (400 MHz, DMSO-d_6) δ: 12.05 (bs, 1H, indole NH, D_2O exchangeable), 8.67 (s, 1H, -N = CH–), 8.33 (d, J = 1.6 Hz, 1H, ArH), 8.13 (s, 1H, indole (C-2) H), 7.91 (bs, 1H, NH, D_2O exchangeable), 7.79 (bs, 1H, NH, D_2O exchangeable), 7.49 (d, J = 8.4 Hz, 1H, ArH), 7.38 (dd, J = 8.8, 2.0 Hz, 1H, ArH), 4.03 (s, 3H, NCH_3), 2.64 (t, J = 7.2 Hz, 2H, CH_2), 1.72–1.58 (m, 2H, CH_2), 0.91 (t, J = 7.2 Hz, 3H, CH_3); ^{13}C NMR (100 MHz, DMSO-d_6) δ: 161.1 (C═O), 157.1, 140.2, 136.0, 135.2, 133.2, 126.9, 126.1, 125.5, 123.1, 114.4, 114.2, 114.0, 39.3 (NMe), 28.0 (CH_2), 21.4 (CH_2), 13.9 (Me); HPLC: 96.8%, Column: X-Bridge C-18 150*4.6 mm 5 μm, mobile phase A: 5 mM Ammonium acetate in water, mobile phase B: CH_3CN, (gradient) T/B% : 0/10, 23/90, 30/90, 31/10, 35/10; flow rate: 1 mL/min, Diluent: CH_3CN: water (80:20), UV: 225.0 nm, retention time 14.4 min; MS (ES mass): *m/z* 388.0 (M+, 98%), 390.0 (M + 2, 100%).

*4.1.13. (E)-4-[{(5-Bromo-1-methyl-1H-indol-3-yl)methylene}amino]-1-methyl-3-propyl-1H-pyrazole-5-carboxamide **(3k)***

White solid (85% yield); mp: 200–202 °C; R_f = 0.25 (40% EtOAc/*n*-hexane); ^{1}H NMR (400 MHz, DMSO-d_6) δ: 8.64 (s, 1H, -N = CH–), 8.33 (d, J = 1.6 Hz, 1H, ArH), 8.11 (s, 1H, indole (C-2) H), 7.87 (d, J = 17.22 Hz, 1H bs, 1H, indole NH, D_2O exchangeable), 7.79 (s, 1H bs, 1H, indole NH, D_2O exchangeable), 7.56 (d, J = 8.8 Hz, 1H, ArH), 7.44 (dd, J = 8.8, 2.0 Hz, 1H, ArH), 4.03 (s, 3H, NCH_3), 3.87 (s, 3H, NCH_3), 2.64 (t, J = 7.2 Hz, 2H, CH_2), 1.70–1.59 (m, 2H, CH_2), 0.92 (t, J = 7.2 Hz, 3H, CH_3); ^{13}C NMR (100 MHz, DMSO-d_6) δ: 161.1 (C═O), 156.5, 140.3, 138.4, 136.6, 133.2, 126.9, 126.4, 125.5, 123.1, 114.4, 113.1, 112.9, 39.3 (NMe), 33.2 (NMe), 28.1 (CH_2), 21.4 (CH_2), 14.0 (Me); HPLC: 99.5%, Column: Eclipse XDB 150*4.6 μm, mobile phase A: 5 mM Ammonium acetate in water, mobile phase B: CH_3CN, (gradient) T/B% : 0/5, 20/90, 30/90, 31/5, 35/5; flow rate: 1 mL/min, Diluent: CH_3CN: water (80:20), UV: 220.0 nm, retention time 13.5 min; MS (ES mass): *m/z* 402.0 (M+, 99%), 404.0 (M + 2, 100%).

*4.1.14. (E)-4-[{(5-bromo-1-ethyl-1H-indol-3-yl)methylene}amino]-1-methyl-3-propyl-1H-pyrazole-5-carboxamide **(3l)***

White solid (81% yield); mp: 164–166 °C; R_f = 0.3 (40% EtOAc/*n*-hexane); ^{1}H NMR (400 MHz, DMSO-d_6) δ: 8.64 (s, 1H, -N = CH–), 8.35 (d, J = 1.6 Hz, 1H, ArH), 8.18 (s, 1H, indole (C-2) H), 7.89 (bs, 1H, NH, D_2O exchangeable), 7.79 (bs, 1H, NH, D_2O exchangeable), 7.62 (d, J = 8.75 Hz, 1H, ArH), 7.43 (dd, J = 8.73, 1.97 Hz, 1H, ArH), 4.28 (q, J = 7.2 Hz, 2H, NCH_2), 4.03 (s, 3H, NCH_3), 2.63 (t, J = 7.2 Hz, 2H, CH_2), 1.70–1.59 (m, 2H, CH_2), 1.41 (t, J = 7.2 Hz, 3H, CH_3), 0.92 (t, J = 7.2 Hz, 3H, CH_3); ^{13}C NMR (100 MHz, DMSO-d_6) δ: 161.1 (C═O), 156.5, 140.3, 136.9, 135.6, 133.2, 126.9, 126.6, 125.5, 123.3, 114.3, 113.3, 112.9, 41.1 (NCH_2), 39.2 (NMe), 28.0 (CH_2), 21.4 (CH_2), 15.0 (Me), 13.9 (Me); HPLC: 96.9%, Column: X-Bridge C-18 150*4.6 mm 5 μm, mobile phase A: 5 mM Ammonium acetate in water, mobile phase B: CH_3CN, (gradient) T/B% : 0/5, 20/90, 30/90, 31/5, 35/5; flow rate: 1 mL/min, Diluent: CH_3CN: water (80:20), UV: 225.0 nm, retention time 16.4 min; MS (ES mass): *m/z* 417.1 (M + 2, 100%).

*4.1.15. (E)-4-{(4-hydroxybenzylidene)amino}-1-methyl-3-propyl-1H-pyrazole-5-carboxamide **(3p)*** [45e]

White solid (77% yield); R_f = 0.22 (40% EtOAc/*n*-hexane); ^{1}H NMR (400 MHz, DMSO-d_6) δ: 10.18 (bs, 1H, OH, D_2O exchangeable), 8.46 (s, 1H, -N = CH–), 7.99 (bs, 1H, NH, D_2O exchangeable), 7.72 (d, J = 8.0 Hz, 2H, ArH), 7.68 (bs, 1H, NH, D_2O exchangeable), 6.87 (d, J = 8.0 Hz, 2H, ArH), 4.00 (s, 3H, NCH_3), 2.63 (t, J = 7.6 Hz, 2H, CH_2), 1.64–1.56 (m, 2H, $MeCH_2$), 0.89 (t, J = 7.2 Hz, 3H, CH_3); ^{13}C NMR (100 MHz, DMSO-d_6) δ: 161.5 (C═O), 161.4, 160.8, 140.8, 131.9, 130.8 (2C), 128.3, 127.7, 116.3 (2C), 39.3 (NMe), 28.3 (CH_2), 21.5 (CH_2), 14.4 (Me); IR (KBr) ν_{max} 3363, 1901, 1657, 1591 cm^{-1}; MS (ES mass): *m/z* 286.9 (M+, 100%).

*4.1.16. 5-(5-Bromo-1-ethyl-1H-indol-3-yl)-1-methyl-4-(prop-2-yn-1-yl)-3-propyl-5,6-dihydro-1H-pyrazolo[4,3-d]pyrimidin-7(4H)-one **(4a)***

White solid (85% yield); mp: 128–132 °C; R_f = 0.23 (40% EtOAc/*n*-hexane); ^{1}H NMR (400 MHz, DMSO-d_6) δ: 8.43 (d, J = 3.6 Hz, 1H, NH, D_2O exchangeable), 8.07 (d, J = 1.6 Hz, 1H, ArH), 7.39 (d, J = 8.8 Hz, 1H, ArH), 7.25–7.16 (m, 2H, indole (C-2) H, ArH), 5.93 (d, J = 2.8 Hz, 1H, CH), 4.12 (t, J = 7.2 Hz, 2H, NCH_2), 3.90 (s, 3H, NCH_3), 3.88–3.75 (m, 2H, alkyne NCH_2), 3.31–3.29 (t, J = 2.4 Hz, 1H, HC≡C), 2.56–2.42 (m, 2H, CH_2), 1.61–1.45 (m, 2H, CH_2), 1.26 (t, J = 7.2 Hz, 3H, CH_3), 0.74 (t, J = 7.2 Hz, 3H, CH_3); ^{13}C NMR (100 MHz, DMSO-d_6) δ: 157.6 (C═O), 141.6, 134.7, 131.0, 128.0, 127.6, 126.3, 123.7, 122.7, 114.1, 111.8, 111.5, 80.2 (-C≡), 75.9 (HC≡), 68.7 (CH), 41.9 (NCH_2), 40.4 (NCH_2), 37.6 (NMe), 27.7 (CH_2), 21.0 (CH_2), 15.2 (Me), 13.7 (Me); HPLC: 97.5%, Column: X-Bridge C-18 150*4.6 mm 5 μm, mobile phase A: 5 mM Ammonium acetate in water, mobile phase B: CH_3CN, (gradient) T/B% : 0/10, 23/90, 30/90, 31/10, 35/10; flow rate: 1 mL/min, Diluent: CH_3CN: water (80:20), UV: 220.0 nm, retention time 17.5 min; MS (ES mass): *m/z* 454.0 (M+, 98%), 456.0 (M + 2, 100%).

*4.1.17. 5-(1-Butyl-1H-indol-3-yl)-1-methyl-4-(prop-2-yn-1-yl)-3-propyl-5,6-dihydro-1H-pyrazolo[4,3-d]pyrimidin-7(4H)-one **(4b)***

White solid (83% yield); mp: 100–102 °C; R_f = 0.41 (40% EtOAc/*n*-hexane); ^{1}H NMR (400 MHz, DMSO-d_6) δ: 8.36 (d, J = 3.6 Hz, 1H, NH, D_2O exchangeable), 7.85 (d, J = 8.0 Hz, 1H, ArH), 7.38 (d, J = 8.4 Hz, 1H, ArH), 7.14–7.06 (m, 2H, indole (C-2) H, ArH), 7.04–6.98 (m, 1H, ArH), 5.96 (d, J = 2.8 Hz, 1H, CH), 4.08 (t, J = 6.8 Hz, 2H, NCH_2), 3.90 (s, 3H, NCH_3), 3.88–3.75 (m, 2H, alkyne NCH_2), 3.28 (t, J = 2.4 Hz, 1H, HC≡C), 2.49–2.37 (m, 2H, CH_2), 1.67–1.58 (m, 2H, CH_2), 1.56–1.44 (m, 2H, CH_2), 1.18–1.07 (m, 2H, CH_2), 0.81 (t, J = 7.2 Hz, 3H, CH_3), 0.69 (t, J = 7.2 Hz, 3H, CH_3); ^{13}C NMR (100 MHz, DMSO-d_6) δ: 157.9 (C═O), 141.4, 136.3, 131.3, 127.5, 126.2, 125.9, 121.3, 120.2, 118.6, 113.5, 109.8, 80.2 (-C≡), 75.8 (HC≡), 68.9 (CH), 45.1 (NCH_2), 41.5 (NCH_2), 37.6 (NMe), 31.7 (CH_2),

27.7 (CH_2), 21.0 (CH_2), 19.3 (CH_2), 13.5 (Me), 13.4 (Me); HPLC: 99.6%, Column: X-Bridge C-18 150*4.6 mm 5 μm, mobile phase A: 5 mM Ammonium acetate in water, mobile phase B: CH_3CN, (gradient) T/B% : 0/5, 20/90, 30/90, 31/5, 35/5; flow rate: 1 mL/min, Diluent: CH_3CN: water (80:20), Max Plot, retention time 17.0 min; MS (ES mass): *m/z* 404.2 (M + 1, 100%).

*4.1.18. 5-(1-Benzyl-1H-indol-3-yl)-1-methyl-4-(prop-2-yn-1-yl)-3-propyl-5,6-dihydro-1H-pyrazolo[4,3-d]pyrimidin-7(4H)-one (**4c**)*

White solid (80% yield); mp: 120–122 °C; R_f = 0.41 (40% EtOAc/*n*-hexane); ^{1}H NMR (400 MHz, DMSO-d_6) δ: 8.40 (d, *J* = 3.60 Hz, 1H, NH, D_2O exchangeable), 7.88 (d, *J* = 7.6 Hz, 1H, ArH), 7.36 (d, *J* = 8.0 Hz, 1H, ArH), 7.28–7.20 (m, 4H, indole (C-2) H, ArH), 7.10–6.99 (m, 4H, ArH), 5.98 (d, *J* = 2.8 Hz, 1H, CH), 5.34 (s, 2H, Benzyl CH_2), 3.89 (s, 3H, NCH_3), 3.88–3.77 (m, 2H, alkyne NCH_2), 3.28 (t, *J* = 2.4 Hz, 1H, HC≡C), 2.48–2.37 (m, 2H, CH_2), 1.56–1.44 (m, 2H, CH_2), 0.67 (t, *J* = 7.2 Hz, 3H); ^{13}C NMR (100 MHz, DMSO-d_6) δ: 157.8 (C═O), 141.5, 138.1, 136.5, 131.2, 128.4 (2C), 127.9, 127.3, 126.8 (2C), 126.3, 126.1, 121.5, 120.3, 118.9, 114.4, 110.2, 80.2 (-C≡), 75.8 (HC≡), 68.9 (CH), 48.8 (NCH_2), 41.7 (NCH_2), 37.6 (NMe), 27.7 (CH_2), 20.9 (CH_2), 13.5 (Me); HPLC: 93.3%, Column: X-Bridge C-18 150*4.6 mm 5 μm, mobile phase A: 5 mM Ammonium acetate in water, mobile phase B: CH_3CN, (gradient) T/B% : 0/10, 23/90, 30/90, 31/10, 35/10; flow rate: 1 mL/min, Diluent: CH_3CN: water (80:20), UV: 225.0 nm, retention time 17.6 min; MS (ES mass): *m/z* 438.2 (M + 1, 100%).

5. Docking study

All ligand structures were drawn in MarvinSketch [46]. Proteins (PDB ID: 6BQG, 4IB4, and 6A94 for $5HT_{2C}$R, $5HT_{2B}$R, and $5HT_{2A}$R respectively) as well as all ligands were prepared (involving optimization, charge calculation, deletion of co-crystal ligand, and addition of hydrogen etc.) using AutoDock tool [47]. All ligands were docked at orthosteric binding site using reliable open-source tool AutoDock Vina [21]. The grid map was made up of 20X20X20 points using AutoGrid with 21.13, 31.33, and 58.50 for $5HT_{2C}$ (for $5HT_{2A}$ 13.42, −1.75, 59.47 and for $5HT_{2B}$ 20.37, 19.14, 11.72) as center_X, center_Y, and center_Z respectively. To search all possible conformation of ligands thoroughly, exhaustiveness value of 20 were used. Though the process was somewhat lengthy or time consuming however this allowed to identify the energetically most favorable pose of individual ligand more accurately. To check the reproducibility of docking result, the docking of each individual ligand was performed at least for five times and maximum difference was found to be ± 0.2. The validation of docking protocol was carried out by re-docking the co-crystal ligand of respective protein structures and calculating the RMSD difference between co-crystal one and docked one in PyMOL [48]. The RMSD values < 2 Å suggested accuracy of the docking protocol used.

6. Pharmacology

6.1. Culture and maintenance of HEK293T cells

HEK293T cells were grown in DMEM supplemented with 10% FBS and 1X antibiotics (Penicillin/Streptomycin). Cells were maintained in 37 °C incubator (5% CO_2 and 95% humidity).

6.2. Reagents and compound preparation

Serotonin and Lorcaserin was purchased from sigma. The d-Luciferin (LUCNA-250) was purchased from Gold Biotech. All compounds were dissolved in DMSO at a concentration of 1 mM. To test compounds for agonist activity, compounds were diluted in 1 mM stock to prepare dose response (serially starting from 1 mM to 0.001 nM) and were added in quadruplicate to the assay plate followed by 12 h incubation. For assessing PAM activity, compounds were added at a concentration of 10 μM, in quadruplicate followed by addition of serotonin at 10 μM concentration to the assay plate and then incubation for 12 h.

6.3. Luciferase assay

For NFAT-RE luciferase assay [40,41], HEK 293 T cells were transiently transfected by mixing branched PEI (1 μg/μl) transfection reagent with 0.1 μg DNA/well of 5-HT_{2C} or 5-HT_{2B} or $5HT_{2A}$ plasmid (GenScript Biotech) and 0.1 μg DNA/well of NFAT-RE luciferase (luc2P/NFAT-RE/Hygro, Promega Corp.) plasmid (DNA:PEI ratio 1:5) and plating (30,000 cells/well) in 96 well plates in 100 μL of culture medium. All primary screening of synthetic compounds was performed at the final concentration of 10 μM (once in quadruplicate). To measure agonist or PAM activity, compounds were added at desired concentration and incubated for 12 h. Post-treatment, luciferase activity was measured via addition of luciferase assay substrate solution using luminometer (Titertek-Berthold). The experiments were performed for three times. The relative luminescence unit (RLU) values were obtained and the data were analyzed through non-linear regression fitting using GraphPad Prism 6.

7. Computational ADME prediction

7.1. Software and methods

The ADME predictions were performed by using the SwissADME web-tool [43], where the molecules were drawn using Marvin JS (version 16.4.18, 2016) and converted into SMILES by JChem Web Services (version 14.9.29, 2013). Then the 3D conformations were generated through the StringMolExport function. All descriptors and important molecular parameters of physicochemical properties were computed by OpenBable API (version 2.3.0, 2012). The predictive models were mostly generated by Quantitative Structure-Property Relationship (QSPR) methods along with some other robust models. As the SwissADME is a web-based tool, all these process are done in an automated manner.

8. Locomotor activity assay

8.1. Experimental design

Larvae developmental stage used for the study: 6 dpf
Embryos used per concentration: 48 embryos
Behavior recording time: 10 min

8.2. Method

The locomotor activity was conducted using the 6 dpf larvae. The total distance (mm) moved in 10 min was measured by using ZebraLab software (Videotrack; ViewPoint Life Sciences, Lyon, France). The larvae were incubated with appropriate drug concentration in 96 well plate one larvae per well. The larvae were acclimatized for 15 min inside the zebrabox and the total distance was calculated by tracking the larvae for 10 min using a high speed infrared camera. The locomotor activity was calculated for the control, serotonin, Lorcaserin and two test compounds and the difference in the total movement were compared between control and the treatment groups using graph pad prism software. The statistical difference between the groups are indicated with asterisks (*P < 0.05; **P < 0.01; ***P < 0.001).

9. BBB penetration prediction

The BBB penetration of test compounds was predicted using BBB Predictor tool (http://www.cbligand.org/BBB/) of AlzPlatform [45]. The threshold score of BBB penetration in this tool is 0.02. The predictor was built by taking 1593 reported compounds as input to develop support vector machine (SVM) algorithm based prediction.

10. *In vitro* metabolic stability in rat liver microsomes

10.1. Experimental design

Metabolic stability was carried out using the mouse liver microsomes. The final composition of the assay included 5 μM of test items (compound **3b** and **3i**) or control item (Diclofenac), 0.25 mg/mL microsomal protein and cofactors (5.0 mM G-6-P, 0.06 U/mL G-6-PDH, 2.0 mM $MgCl_2$, 1.0 mM $NADP^+$). The final concentration of DMSO in the incubation mixture was 0.1%. Test item/ Control items were incubated with mouse liver microsomes in presence and absence of cofactors. The reaction mixture (100 μL) was removed at specified time period and the reaction was stopped by addition of stop solution. The samples were extracted in presence of internal standard and were analyzed using LC-MS/MS. The percent of the test/Control item remaining after specified incubation period was calculated with respect to the peak area ratio at time 0 min.

10.2. Brief protocol

The 4X working concentration of test item (20 μM)/Control items (20 μM) were prepared in 50 mM Potassium phosphate buffer (pH 7.4) using 5 mM DMSO stocks. The 10X working concentration of mouse liver microsomal solution (2.5 mg/mL) was prepared in 50 mM Potassium phosphate buffer (pH 7.40) using stock solution of mouse liver microsomes (20 mg/mL protein concentration). The reaction mixture of 100 μL (for each time point) was incubated by adding 45 μL potassium phosphate buffer, 10 μL of diluted mouse liver microsomal solution (2.5 mg/mL), 25 μL of test/control items (20 μM) and 20 μL of Cofactors/Buffer. The reaction mixture was incubated further at 37 °C for specified incubation time points (With Cofactors: 0, 15, 30, 60 and 120 min; Without Cofactors: 0 and 120 min). A 100 μL incubation samples of test items and Control items at specified incubation time points were transferred to respective tubes for sample extraction.

10.3. Protein precipitation extraction method

Test and Control items specimens were extracted by Protein precipitation method. A 100 μL of incubation sample at each time point was added to tubes containing 200 μL of ice cold Acetonitrile and 10 μL Internal standard (Minoxidil at 5 μg/mL). Then the tubes were vortex mixed thoroughly and centrifuged at 10000 rpm for 10 min at 4 °C. A clear supernatant of 200 μL of samples were submitted for LC- MS/MS analysis.

Declaration of Competing Interest

The authors declare that they have no known competing financial interests or personal relationships that could have appeared to influence the work reported in this paper.

Acknowledgements

GSR thanks DST, India for a INSPIRE fellowship (IF160590). Authors thank the Management of DRILS, Hyderabad, India for encouragement and support and DST-DPRP, New Delhi, India for financial assistance [Grant No. VI-D&P/565/2016-17/TDT (G1)].

Appendix A. Supplementary data

Supplementary data to this article can be found online at https://doi.org/10.1016/j.bioorg.2021.105380.

References

[1] B. Benhamu, M. Martin-Fontecha, H. Vazquez-Villa, L. Pardo, M.L. Lopez-Rodriguez, Serotonin 5-HT_6 receptor antagonists for the treatment of cognitive deficiency in Alzheimer's disease, J. Med. Chem. 57 (2014) 7160–7181.
[2] B.J. Sargent, A.J. Henderson, Targeting 5-HT receptors for the treatment of obesity, Curr. Opin. Pharmacol. 11 (2011) 52–58.
[3] J.C.G. Halford, J.A. Harrold, C.L. Lawton, J.E. Blundell, Serotonin (5-HT) drugs: effects on appetite expression and use for the treatment of obesity, Curr. Drug Targets 6 (2005) 201–213.
[4] G. Di Giovanni, P. De Deurwaerdere, New therapeutic opportunities for 5-HT2C receptor ligands in neuropsychiatric disorders, Pharmacol. Ther. 157 (2016) 125–162.
[5] N.H. Jensen, T.I. Cremers, F. Sotty, Therapeutic potential of 5-HT2C receptor ligands, Sci. World J. 10 (2010) 1870–1885.
[6] G.A. Higgins, E.M. Sellers, P.J. Fletcher, From obesity to substance abuse: therapeutic opportunities for 5-HT2C receptor agonists, Trends Pharmacol. Sci. 34 (2013) 560–570.
[7] J. Lee, M.E. Jung, J. Lee, 5-HT2C receptor modulators: a patent survey, Expert Opin. Ther. Pat. 20 (11) (2010) 1429–1455.
[8] A.S. Garfield, L.K. Heisler, Pharmacological targeting of the serotonergic system for the treatment of obesity, J. Physiol. 587 (2009) 49–60.
[9] N.J.T. Monck, G.A. Kennett, 5-HT_{2C} Ligands: recent progress, Prog. Med. Chem. 46 (2008) 281–390.
[10] S.R. Smith, W.A. Prosser, D.J. Donahue, M.E. Morgan, C.M. Anderson, W.R. Shanahan, A.S. Group, Lorcaserin (APD356), a selective 5-HT(2C) agonist, reduces body weight in obese men and women, Obesity 17 (2009) 494–503.
[11] C.K. Martin, L.M. Redman, J. Zhang, M. Sanchez, C.M. Anderson, S.R. Smith, E. Ravussin, Lorcaserin, a 5-HT2C receptor agonist, reduces body weight by decreasing energy intake without influencing energy expenditure, J. Clin. Endocrinol. Metab. 96 (2011) 837–845.
[12] J.B. Cohen, K.M. Gadde, Weight loss medications in the treatment of obesity and hypertension, Curr. Hypertens. Rep. 21 (2019) 16.
[13] a) E. A. Bohula, S. D. Wiviott, D. K. McGuire, S. E. Inzucchi, J. Kuder, K. Im, C. L. Fanola, A. Qamar, C. Brown, A. Budaj, A. Garcia-Castillo, Cardiovascular safety of lorcaserin in overweight or obese patients. N. Engl. J. Med. 379 (2018) 1107-1117. b) J. J. DiNicolantonio, S. Chatterjee, J. H. O'Keefe, P. Meier, Lorcaserin for the treatment of obesity? A closer look at its side effects. Open Heart (2014), http://doi.org/10.1136/openhrt-2014-000173.
[14] FDA requests withdrawal of lorcaserin from US market. Reactions Weekly 1792 (2020) 1. https://doi.org/10.1007/s40278-020-75109-8.
[15] W.K. Kroeze, B.L. Roth, The molecular biology of serotonin receptors: therapeutic implications for the interface of mood and psychosis, Biol. Psychiatry. 44 (1998) 1128–1142.
[16] D. Hoyer, J.P. Hannon, G.R. Martin, Molecular, pharmacological and functional diversity of 5-HT receptors, Pharmacol. Biochem. Behav. 71 (4) (2002) 533–554.
[17] R.B. Rothman, M.H. Baumann, J.E. Savage, L. Rauser, A. McBride, S.J. Hufeisen, B.L. Roth, Evidence for possible involvement of 5-HT2B receptors in the cardiac valvulopathy associated with fenfluramine and other serotonergic medications, Circulation 102 (2000) 2836–2841.
[18] a) J. García-Cárceles, J. M. Decara, H. Vázquez-Villa, R. Rodríguez, E. Codesido, J. Cruces, J. Brea, M. I. Loza, F. Alén, J. Botta, P. J. McCormick, J. A. Ballesteros, B. Benhamú, F. R. de Fonseca, M. L. López-Rodríguez, A Positive Allosteric Modulator of the Serotonin 5-HT2C Receptor for Obesity. J. Med. Chem. 60 (2017) 9575−9584. b) M. Toro-Sazo, J.´Brea, M. I. Loza, M. Cimadevila, B. K. Cassels, 5-HT2 receptor binding, functional activity and selectivity in N-benzyltryptamines. PLoS ONE 14 (2019): e0209804. https://doi.org/10.1371/journal.pone.0209804. c) M. R Braden, J. C. Parrish, J. C. Naylor, D. E. Nichols, Molecular interaction of serotonin 5-HT2A receptor residues Phe339(6.51) and Phe340(6.52) with superpotent N-benzyl phenethylamine agonists. Mol. Pharmacol. 70 (2006) 1956-1964; http://doi.org/10.1124/mol.106.028720.
[19] a) K. K. -C. Liu, B. A. Lefker, M. A. Dombroski, P. Chiang, P. Cornelius, T. A. Patterson, Y. Zeng, S. Santucci, E. Tomlinson, C. P. Gibbons, R. Marala, J. A. Brown, J. X. Kong, E. Lee, W. Werner, Z. Wenzel, C. Giragossian, H. Chen, S. B. Coffey, Orally active and brain permeable proline amides as highly selective 5HT2c agonists for the treatment of obesity. Bioorg. Med. Chem. Lett. 20 (2010) 2365–2369. b) J. Carpenter, Y. Wang, G. Wu, J. Feng, X. -Y. Ye, C. L. Morales, M. Broekema, K. A. Rossi, K. J. Miller, B. J. Murphy, G. Wu, S. E. Malmstrom, A. V. Azzara, P. M. Sher, J. M. Fevig, A. Alt, R. L. Bertekap Jr, M. J. Cullen, T. M. Harper, K. Foster, E. Luk, Q. Xiang, M. F. Grubb, J. A. Robl, D. A. Wacker, Utilization of an active site mutant receptor for the identification of potent and selective atypical 5-HT2C receptor agonists. J. Med. Chem, 60 (2017) 6166–6190.
[20] I. Warad, O. Ali, A.A. Ali, N.A. Jaradat, F. Hussein, L. Abdallah, N. Al-Zaqri, A. Alsalme, F.A. Alharthi, Synthesis and Spectral Identification of Three Schiff Bases with a 2-(Piperazin-1-yl)-N-(thiophen-2-ylmethylene)ethanamine Moiety Acting as Novel Pancreatic Lipase Inhibitors: Thermal, DFT, Antioxidant, Antibacterial, and Molecular Docking Investigations, Molecules 25 (2020) 2253, https://doi.org/10.3390/molecules25092253.
[21] O. Trott, A.J. Olson, AutoDock Vina: improving the speed and accuracy of docking

with a new scoring function, efficient optimization, and multithreading, J. Comput. Chem. 31 (2010) 455–461.
[22] a) Y. Peng, J. D. McCorvy, K. Harpsøe, K. Lansu, S. Yuan, P. Popov, L. Qu, M. Pu, T. Che, L. F. Nikolajsen, X.-P. Huang, Y. Wu, L. Shen, W. E. Bjørn-Yoshimoto, K. Ding, D. Wacker, G. W. Han, J. Cheng, V. Katritch, A. A. Jensen, M. A. Hanson, S. Zhao, D. E. Gloriam, B. L. Roth, R. C. Stevens, Z.-J. Liu. 5-HT2C receptor structures reveal the structural basis of GPCR polypharmacology. Cell 172 (2018) 719-730, http://doi.org/10.1016/j.cell.2018.01.001. b) S. Franchini, L. I. Manasieva, C. Sorbi, U. M. Battisti, P. Fossa, E. Cichero, N. Denora, R. M. Iacobazzi, A. Cilia, L. Pirona, S. Ronsisvalle, G. Aricò, L. Brasili, Synthesis, biological evaluation and molecular modeling of 1-oxa-4-thiaspiro- and 1,4-dithiaspiro[4.5]decane derivatives as potent and selective 5-HT1A receptor agonists. Eur. J. Med. Chem. 125 (2017) 435-452 c) S. Franchini, U. M. Battisti, A. Baraldi, A. Prandi, P. Fossa, E. Cichero, A. Tait, C. Sorbi, G. Marucci, A. Cilia, L. Pirona, L. Brasili, Structure-affinity/activity relationships of 1,4-dioxa-spiro[4.5]decane based ligands at α < alpha > 1 and 5-HT1A receptors. Eur. J. Med. Chem. 87 (2014) 248-266 d) A. Prandi, S. Franchini, L. I. Manasieva, P. Fossa, E. Cichero, G. Marucci, M. Buccioni, A. Cilia, L. Pirona, L. Brasili, Synthesis, biological evaluation, and docking studies of tetrahydrofuran-cyclopentanone- and cyclopentanol-based ligands acting at adrenergic α1- and serotonine 5-HT1A receptors. J. Med. Chem. 55 (2012) 23–36 e) P. Linciano, C. Sorbi, A. Comitato, A. Lesniak, M. Bujalska-Zadrożny, A. Pawłowska, A. Bielenica, J. Orzelska-Górka, E. Kędzierska, G. Biała, S. Ronsisvalle, S. Limoncella, L. Casarini, E. Cichero, P. Fossa, G. Satała, A. J. Bojarski, L Brasili, R. Bardoni, S. Franchini, Identification of a Potent and Selective 5-HT1A Receptor Agonist with In Vitro and In Vivo Antinociceptive Activity. ACS Chem. Neurosci. 11 (2020) 4111-4127.
[23] a) M. M. Sprung, A Summary of the Reactions of Aldehydes with Amines. Chem. Rev. 26 (1940) 297-338. b) H. Liua, Z.-W. Chua, D.-G. Xiaa, H.-Q. Caob, X.-H. Lva, Discovery of novel multi-substituted benzo-indole pyrazole schiff base derivatives with antibacterial activity targeting DNA gyrase. Bioor. Chem. 99 (2020) 103807; https://doi.org/10.1016/j.bioorg.2020.103807 c) B. G. Molina, L. Cianga, A.-D, Bendrea, I. Cianga, L. J. del Valle, Fr. Estrany, C. Alemán, E. Armelin, Amphiphilic polypyrrole-poly(Schiff base) copolymers with poly(ethylene glycol) side chains: synthesis, properties and applications. Polym. Chem., 9 (2018) 4218-4232.
[24] Y. Nishina, Application of heterogeneous catalysts for organic synthesis by controlling the oxidation state of metal species, J. Synthetic Organic Chem. Japan 71 (2013) 1307–1308, https://doi.org/10.5059/yukigoseikyokaishi.71.1307.
[25] S.K. Kumar, J. Iqbal, M. Pal, Amberlyst-15: a mild, efficient and reusable heterogeneous catalyst for N-tert-butoxycarbonylation of amines, Tetrahedron Lett. 50 (2009) 6244–6246.
[26] P.V. Murthy, D. Rambabu, G.R. Krishna, C.M. Reddy, K.R.S. Prasad, M.V.B. Rao, M. Pal, Amberlyst-15 mediated synthesis of 2-substituted 2,3-dihydroquinazolin-4 (1*H*)-ones and their crystal structure analysis, Tetrahedron Lett. 53 (2012) 863–867.
[27] D. Rambabu, P.R.K. Murthi, B. Dulla, M.V.B. Rao, M. Pal, Amberlyst-15 catalyzed synthesis of 2-substituted 1,3-benzazoles in water under ultrasound, Synth. Commun. 43 (2013) 3083–3092.
[28] S.K. Kumar, D. Rambabu, C.V. Kumar, B.Y. Sreenivas, K.R.S. Prasad, M.V.B. Rao, M. Pal, Catalysis by Amberlyst-15 under ultrasound in water: A green synthesis of 1,2,4-benzothiadiazine-1,1-dioxides and their spiro derivatives, RSC Adv. 3 (2013) 24863–24867.
[29] P.R.K. Murthi, D. Rambabu, M.V.B. Rao, M. Pal, Synthesis of substituted pyrroles via Amberlyst-15 mediated MCR under ultrasound, Tetrahedron Lett. 55 (2014) 507–509.
[30] For a review, see R. Pal, T. Sarkar, S. Khasnobis, Amberlyst-15 in organic synthesis. Arkivoc 1 (2012) 570–609.
[31] T.J. Mason, Ultrasound in synthetic organic chemistry, Chem. Soc. Rev. 26 (1997) 443–451.
[32] R. Cella, H. A. Stefani, Ultrasonic Reactions, in Green Techniques for Organic Synthesis and Medicinal Chemistry (eds W. Zhang and B. W. Cue), John Wiley & Sons, Ltd, Chichester, UK. http://doi.org/10.1002/9780470711828.ch13, 2012.
[33] L. Pizzuti, M. S. F. Franco, A. F. C. Flores, F. H. Quina, C. M. P. Pereira, Recent Advances in the Ultrasound-Assisted Synthesis of Azoles, (M. Kidwai, N. K. Mishra), Green Chem. - Environ. Benign Approaches. IntechOpen 2012; http://doi.org/10.5772/35171.
[34] S. Puri, B. Kaur, A. Parmar, H. Kumar, Applications of Ultrasound in Organic Synthesis - A Green Approach, Curr. Org. Chem. 17 (2013) 1790–1828.
[35] D.N.K. Reddy, K.B. Chandrasekhar, Y.S.S. Ganesh, G.R. Reddy, J.P. Kumar, R.K. Kapavarapu, M. Pal, FeF_3-catalyzed MCR in PEG-400: ultrasound assisted synthesis of N-substituted 2-aminopyridines, RSC Adv. 6 (2016) 67212–67217, https://doi.org/10.1039/c6ra14228a.
[36] A.V. Narsaiah, A.R. Reddy, B.V.S. Reddy, J.S. Yadav, Amberlyst-15®: An Efficient, Cost-Effective and Recyclable Hetero Geneous Solid Acid Catalyst for the Synthesis of β-Enaminones and β-Enamino Esters, Open Cat. J. 4 (2011) 43.
[37] X.-S. Wang, K. Yang, J. Zhou, S.-J. Tu, Facile method for the combinatorial synthesis of 2, 2-disubstituted quinazolin-4 (1 H)-one derivatives catalyzed by iodine in ionic liquids, J. Comb. Chem. 12 (2010) 417–421.
[38] A.A. Mohammadi, M. Dabiri, H. Qaraat, A regioselective three-component reaction for synthesis of novel 1′ H-spiro [isoindoline-1, 2′-quinazoline]-3, 4′(3′ H)-dione derivatives, Tetrahedron 65 (2009) 3804–3808.
[39] K.S. Suslick, D.A. Hammerton, R.E. Cline, Sonochemical hot spot, J. Am. Chem. Soc. 108 (1986) 5641–5642.
[40] Z. Cheng, D. Garvin, A. Paguio, P. Stecha, K. Wood, F. Fan, Luciferase reporter assay system for deciphering GPCR pathways, Curr. Chem. Genomics 4 (2010) 84.
[41] a) K. Singh, C. Sona, V. Ojha, M. Singh, A. Mishra, A. Kumar, M. I. Siddiqi, R. P. Tripathi, P. N. Yadav, Identification of dual role of piperazine-linked phenyl cyclopropyl methanone as positive allosteric modulator of 5-HT2C and negative allosteric modulator of 5-HT2B receptors. Eur. J. Med. Chem. 164 (2019) 499-516. b) G. K. Veeramachaneni, V. B. S. C. Thunuguntla, M. Bhaswant, M. L. Mathai, J. S. Bondili, Pharmacophore Directed Screening of Agonistic Natural Molecules Showing Affinity to 5HT2C Receptor. Biomolecules 9 (2019) 556; http://doi.org/10.3390/biom9100556.
[42] A. Aispuro-Pérez, J. López-Ávalos, F. García-Páez, J. Montes-Avila, L.A. Picos-Corrales, A. Ochoa-Terán, P. Bastidas, S. Montaño, L. Calderón-Zamora, U. Osuna-Martínez, J. Sarmiento-Sánchez, Synthesis and molecular docking studies of imines as α-glucosidase and α-amylase inhibitors, Bioorg. Chem. 94 (2020) 103491.
[43] A. Daina, O. Michielin, V. Zoete, SwissADME: a free web tool to evaluate pharmacokinetics, drug-likeness and medicinal chemistry friendliness of small molecules, Sci. Rep. 7 (2017) 42717.
[44] a) C. J. Browne, X. Ji, G. A. Higgins, P. J. Fletcher, C. Harvey-Lewis, Pharmacological Modulation of 5-HT2CReceptor Activity Produces Bidirectional Changes in Locomotor Activity, Responding for a Conditioned Rein forcer, and Mesolimbic DA Release in C57BL/6 Mice. Neuropsychopharmacol.42 (2017) 2178–2187, doi:10.1038/npp.2017.124. b) A. J. Grottick, W. A. Corrigall, G. A. Higgins, Activation of 5-HT(2C) Receptors Reduces the Locomotor and Rewarding Effects of Nicotine. Psychopharmacol. 157 (2001) 292-298; doi: 10.1007/s002130100801. c) A. Griffin, K. R. Hamling, K. Knupp, S. G. Hong, L. P. Lee, S. C. Baraban, Clemizole and modulators of serotonin signalling suppress seizures in Dravet syndrome. Brain. 140 (2017) 669-683; http://doi.org/10.1093/brain/aww342. d) T. Oka, Y. Nishimura, L. Zang, M. Hirano, Y. Shimada, Z. Wang, N. Umemoto, J. Kuroyanagi, N. Nishimura, T. Tanaka, Diet-induced obesity in zebrafish shares common pathophysiological pathways with mammalian obesity. BMC Physiol. 10 (2010) 21; http://doi.org/10.1186/1472-6793-10-21. e) H. Schneider, L. Fritzky, J. Williams, C. Heumann, M. Yochum, K. Pattar, G. Noppert, V. Mock, E. Hawley, Cloning and expression of a zebrafish 5-HT(2C) receptor gene. Gene 502 (2012) 108-117; http://doi.org/10.1016/j.gene.2012.03.070. f) M. Lange, W. Norton, M. Coolen, M. Chaminade, S. Merker, F. Proft, A. Schmitt, P. Vernier, K. P. Lesch, L. Bally-Cuif, The ADHD-susceptibility gene lphn3. 1 modulates dopaminergic neuron formation and locomotor activity during zebrafish development. Mol. Psychiatry 17 (2012) 946-954, http://doi.org/10.1038/mp.2012.29.
[45] a) H. Liu, L. Wang, M. Lv, R. Pei, P. Li, Z. Pei, Y. Wang, W. Su, X.-Q. Xie, ALzPlatform: An Alzheimer's Disease Domain-Specific Chemogenomics Knowledgebase for Polypharmacology and Target Identification Research. J. Comput. Info Modeling. 54 (2014) 1050-1060. http://pubs.acs.org/doi/full/10.1021/ci500004h b) L. Quintieri, M. Fantin, P. Palatini, S. De Martin, A. Rosato, M. Caruso, C. Geroni, M. Floreani, In vitro hepatic conversion of the anticancer agent nemorubicin to its active metabolite PNU-159682 in mice, rats and dogs: A comparison with human liver microsomes. Biochem Pharmacol. 76 (2008) 784–795. c) P. Deng, D. Zhong, K. Yu, Y. Zhang, T. Wang, X. Chen, Pharmacokinetics, Metabolism, and Excretion of the Antiviral Drug Arbidol in Humans. Antimicrob. Agents Chemother. 57 (2013) 1743–1755 d) Z.-Q. Liao, C. Dong, K. E. Carlson, S. Srinivasan, J. C. Nwachukwu, R. W. Chesnut, A. Sharma, K. W. Nettles, J. A. Katzenellenbogen, H. -B. Zhou, Triaryl-Substituted Schiff Bases Are High-Affinity Subtype-Selective Ligands for the Estrogen Receptor. J. Med. Chem. 57 (2014) 3532−3545. e) D. Rambabu, G. R. Krishna, S. Basavoju, C. M. Reddy, M. Pal, Crystal structure and synthesis of 4-(4-hydroxybenzylideneamino)-1-methyl-3-propyl-1H-pyrazole-5-carboxamide. J. Mol. Struct. 994 (2011) 332–334.
[46] P. Csizmadia, MarvinSketch and MarvinView: molecule applets for the World Wide Web. In Proceedings of ECSOC-3, the third international electronic conference on synthetic organic chemistry, September (1999) 1-30 (p. 367-369).
[47] R. Huey, G.M. Morris, AutoDock tools, The Scripps Research Institute, La Jolla, CA, USA, 2003.
[48] W. L. DeLano, Pymol: An open-source molecular graphics tool. CCP4 newsletter on protein, Crystallography 40 (2002) 82-92.